

Evolution of Intermediate Mass Stars

(in particular: why should we care about AGB stars?)



S. Cristallo

Osservatorio Astronomico di Teramo - INAF

Intermediate Mass Stars (IMs)

IMs

Lower mass limit:

Non degenerate He ignition

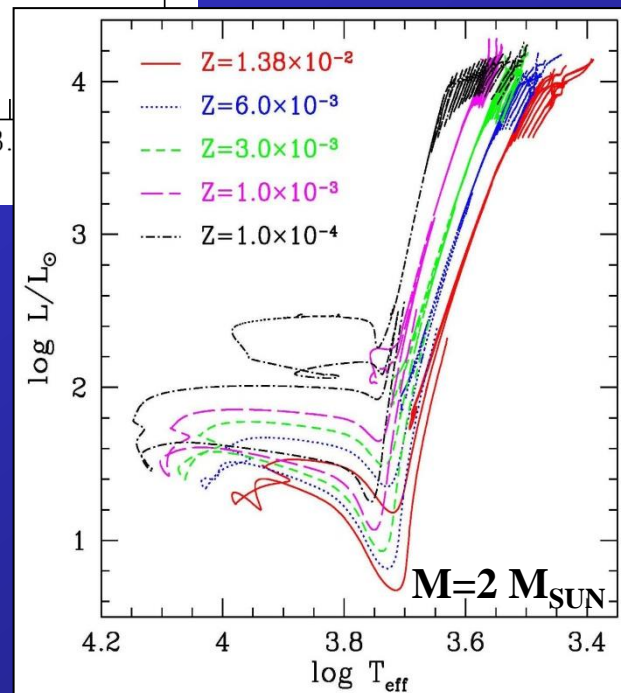
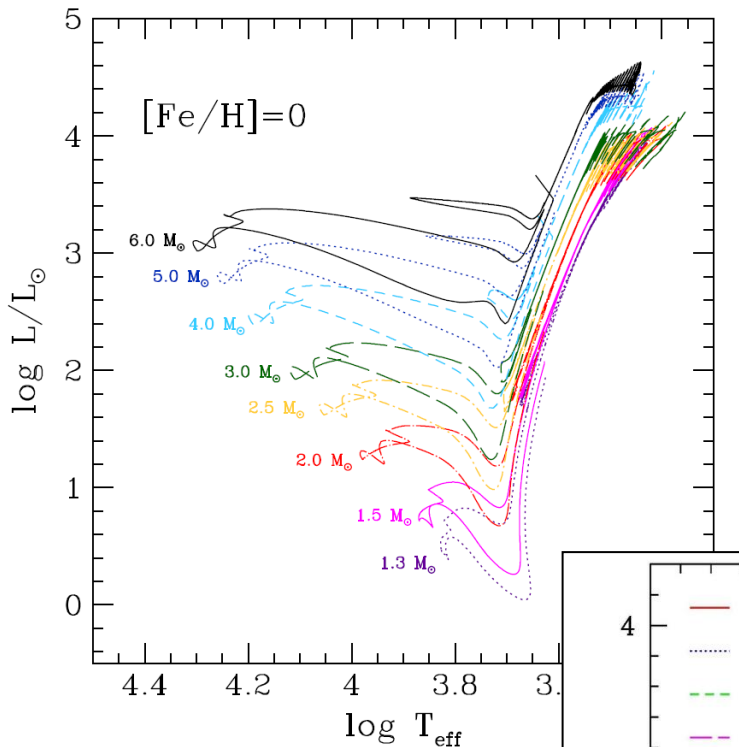
($M_{\text{low}} \approx 1.5 \div 2 M_{\text{SUN}}$)

Upper mass limit:

Partially degenerate CO core

($M_{\text{up}} \approx 8 \div 9 M_{\text{SUN}}$)

For massive AGBs (7-8-9)
see SISS talk



Major uncertainty sources in stellar evolutionary codes

1. **Opacities and Equation of State: $P=P(\rho, T)$;**
2. **Convection (definition of convective borders and treatment of radiative/convective interfaces; mixing efficiency);**
3. **Mass loss law.**
4. **Rotation? Magnetic fields?**

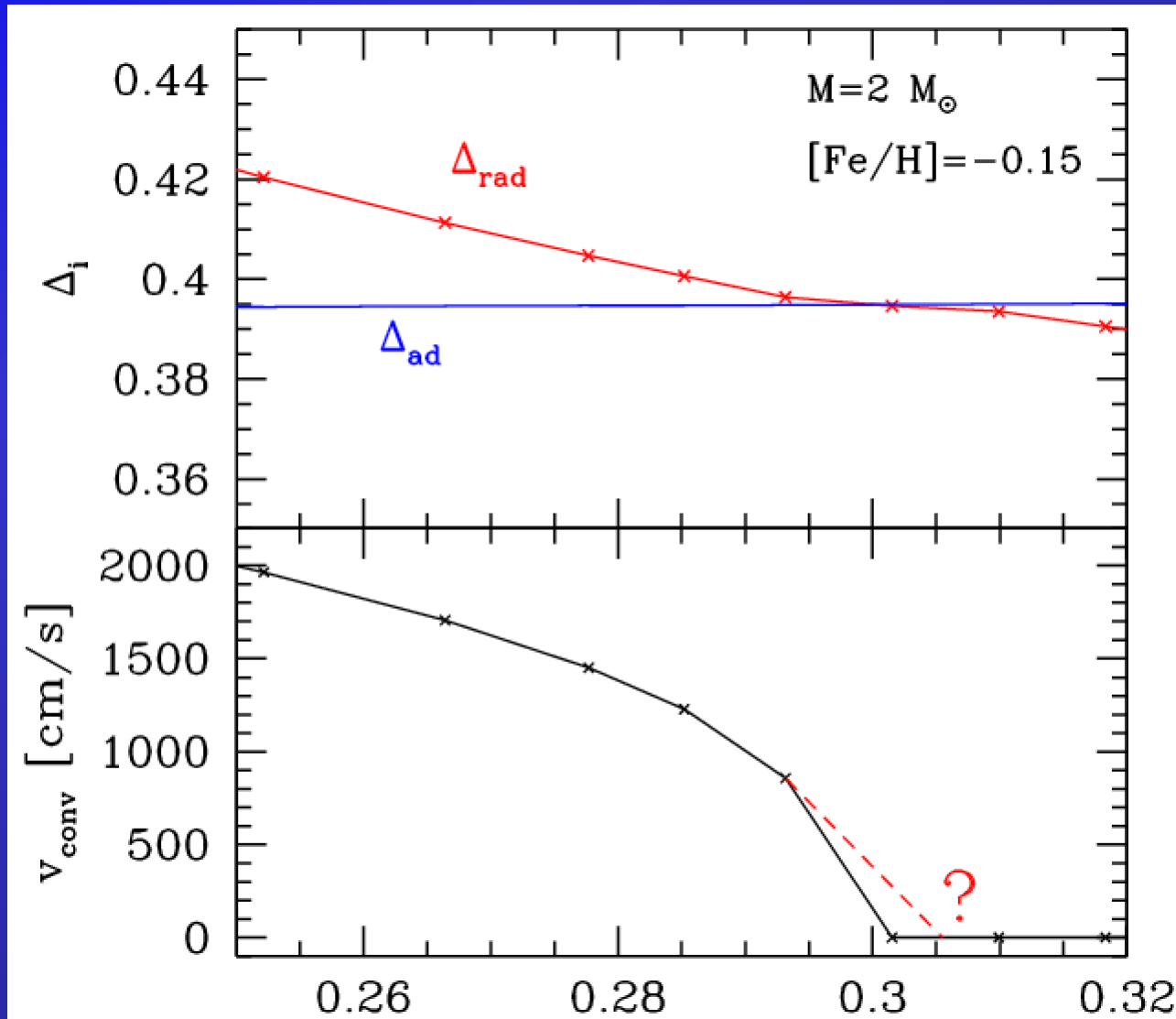
Unfortunately, convection (and rotation) are too complex phenomena to be derived from first principles.

Models can be «guided» by observations, but the question is: should we constrain or calibrate them?

Convection : related problems

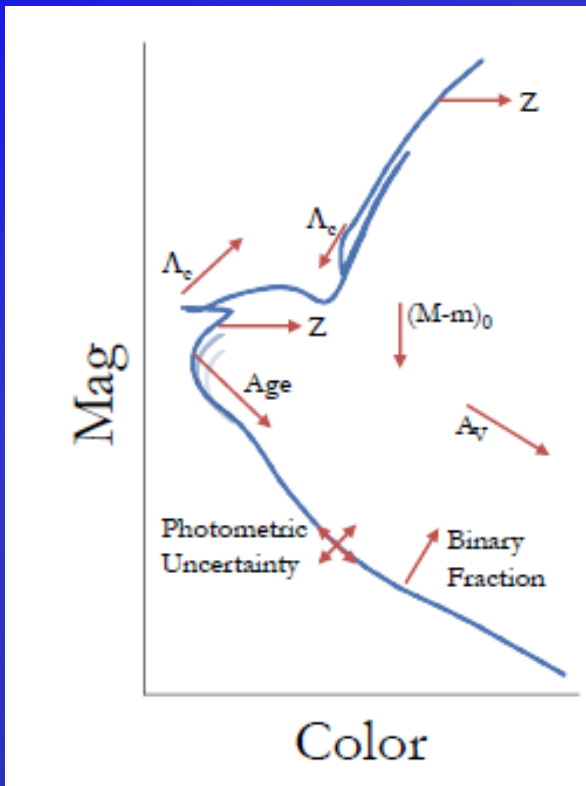
- Determine the position of convective borders
(Bare Schwarzschild criterion? Overshoot? Undershoot?)
- Calculate temperature gradient and velocities inside convective zones
(Mixing length theory? Full Spectrum of Turbulence?)
↓ ↓ ↓
It neglects a fundamental property of turbulence: the non locality of the gradient
- Time dependent convection vs Instantaneous mixing
- Mixing efficiency of chemicals
(Advective approach? Diffusive approach?)

Convective core H burning



Core H-burning overshoot

- More fuel to be burnt during the Main Sequence (MS) phase;
- Higher luminosity during the MS phase (mimicking a younger age), thus there is a sort of Age- Λ_C degeneracy



Λ_C : strength of overshooting (in H_p)

$$0 \leq \Lambda_C \leq 0.5$$

Constant

Variable with mass

Schaller+ 1992
Demarque+ 1994
Sarajedini+ 1999
Woo+ 2003
Mucciarelli+ 2007
Girardi+ 2009
Deheuvels+ 2010
Guenther+ 2014
Yang&Tian 2017

Bressan+ 1993
Claret&Torres 2016

Rosenfield+ 2017

However...

The correct evaluation of the size of an unstable region is primarily dependent on the accuracy of the input physics. For instance, **Dominguez et al. 1999** found that differences between codes WITH or WITHOUT overshoot are of the same order of magnitude as those found between two sets calculated WITHOUT overshoot and different input physics.

NGC 1866 in LMC (Age \approx 150 Myr)

Testa+ 1999 using models by **Straniero+ 1997** find no need for overshoot.

Barmina+ 2002 using models by **Girardi+ 2000** instead need overshoot.

Brocato+ 2003,2004: no overshoot when using Pisa models, but needed if Padua models are used.

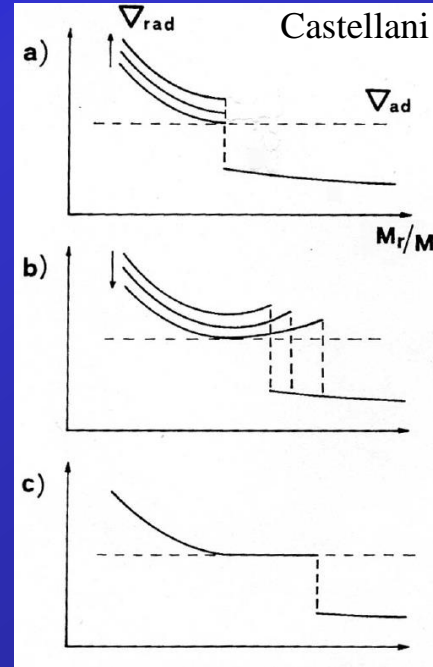
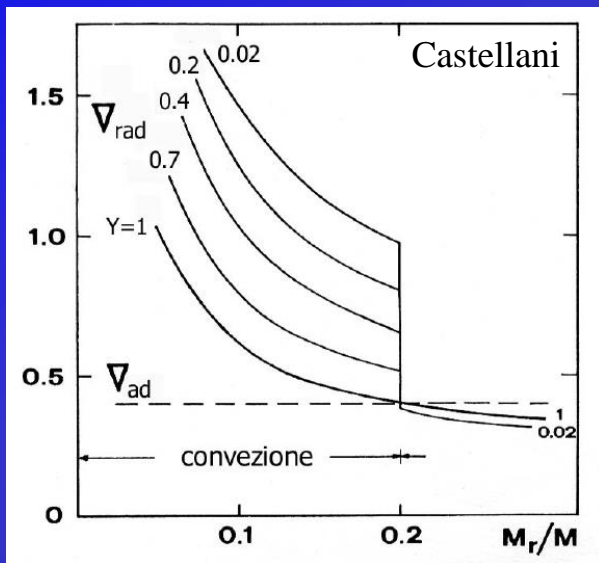
NGC 1978 in LMC (Age \approx 2 Gyr)

Mucciarelli+ 2007a,b: all tested models (Teramo, Pisa, Padova) need overshoot.

Colucci&Bernstein 2012: Teramo isochrones without overshoot produce a more accurate [Fe/H] in their Integrated Light analysis.

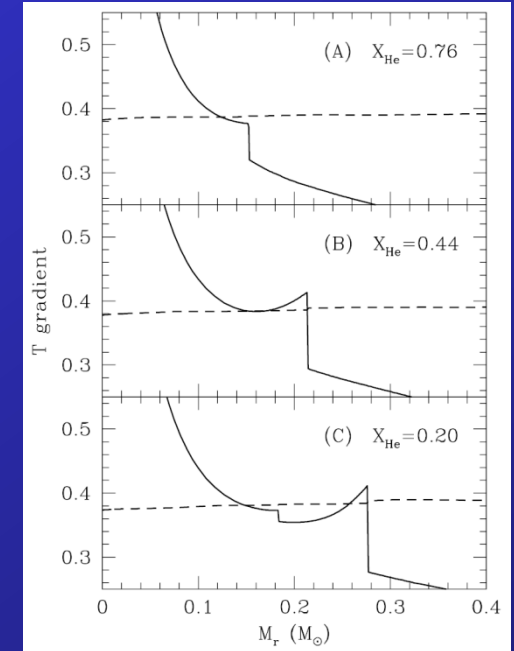
Convective core He burning

In this case, He is converted to C (more opaque) and, in turn, the convective core size must increase (Schwarzschild 1970).



**Induced overshoot
(SEMICONVECTION)**

- Castellani+ 1971
- Sweigart&Demarque 1972
- Iben 1986
- Lattanzio 1991
- Dominguez+ 1999



Mechanical overshoot

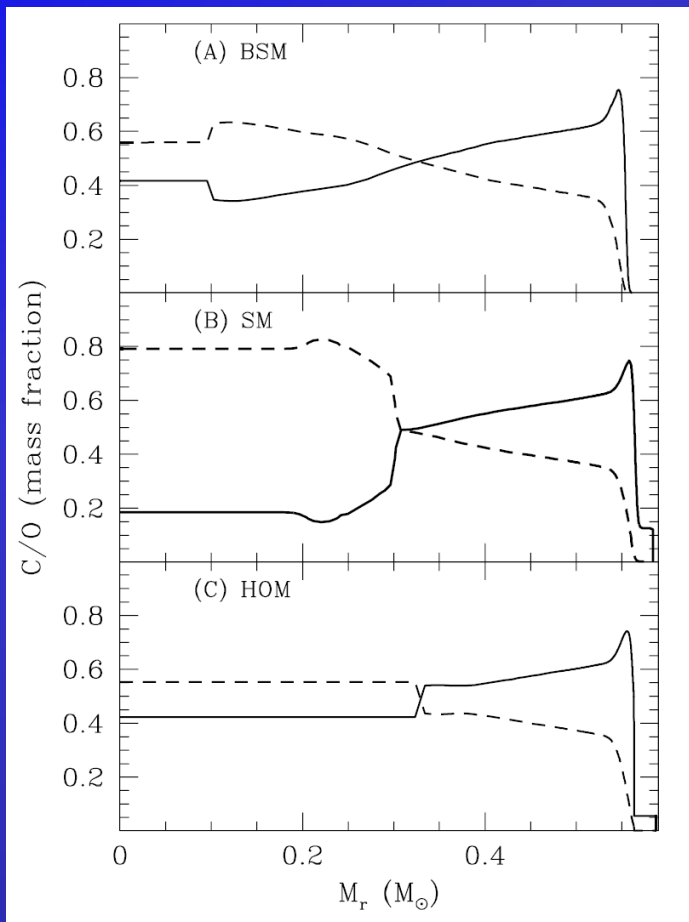
- Shaviv&Salpeter 1973
- Maeder 1975
- Bertelli+ 1990
- Schaller+ 1992
- Bressan+ 1993
- Herwig+ 1997
- Girardi+ 2000

Bare Schwarzschild

- Umeda+ 1999
- Althaus+ 2002

Overshooting vs Semiconvection

Another player: the $^{12}\text{C}(\alpha,\gamma)^{16}\text{O}$



Bare Schwarzschild

Semiconvection

Efficient overshoot

Oxygen central abundance of
the White Dwarf GD358
(Metcalf+ 2001)



Higher $^{12}\text{C}(\alpha,\gamma)^{16}\text{O}$

Standard $^{12}\text{C}(\alpha,\gamma)^{16}\text{O}$

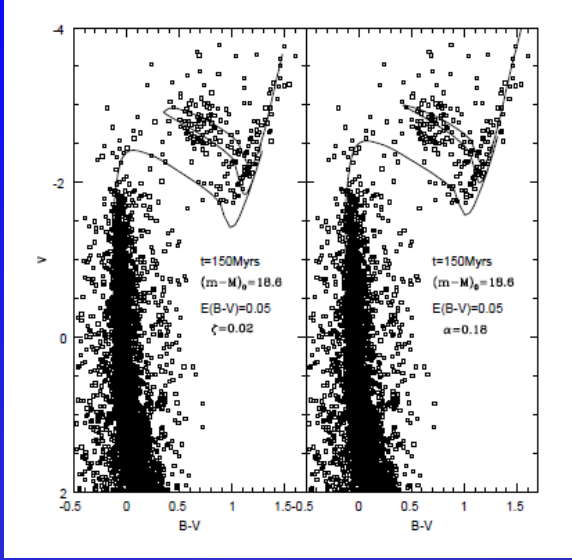
Straniero+ 2003

Diffusive
mixing

Instantaneous
mixing with Λ_c

NGC 1866...again....

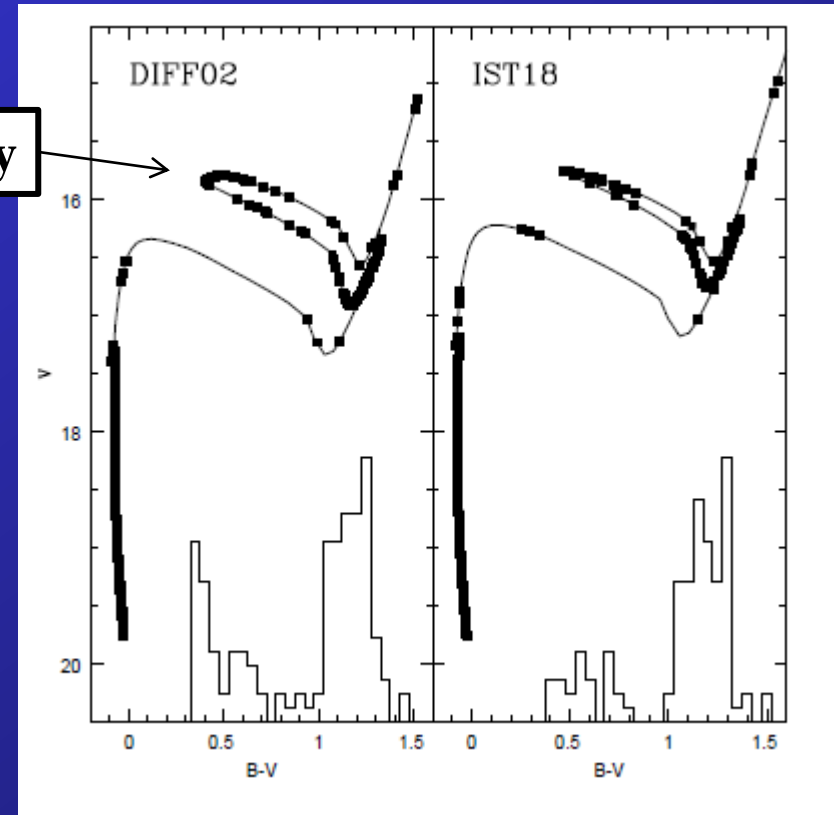
Match the Blue/Red ratio of the stars
in the clump region (≈ 1)



Diffusive
mixing

Instantaneous
mixing with Λ_c

It burns slowly



Core H-burning

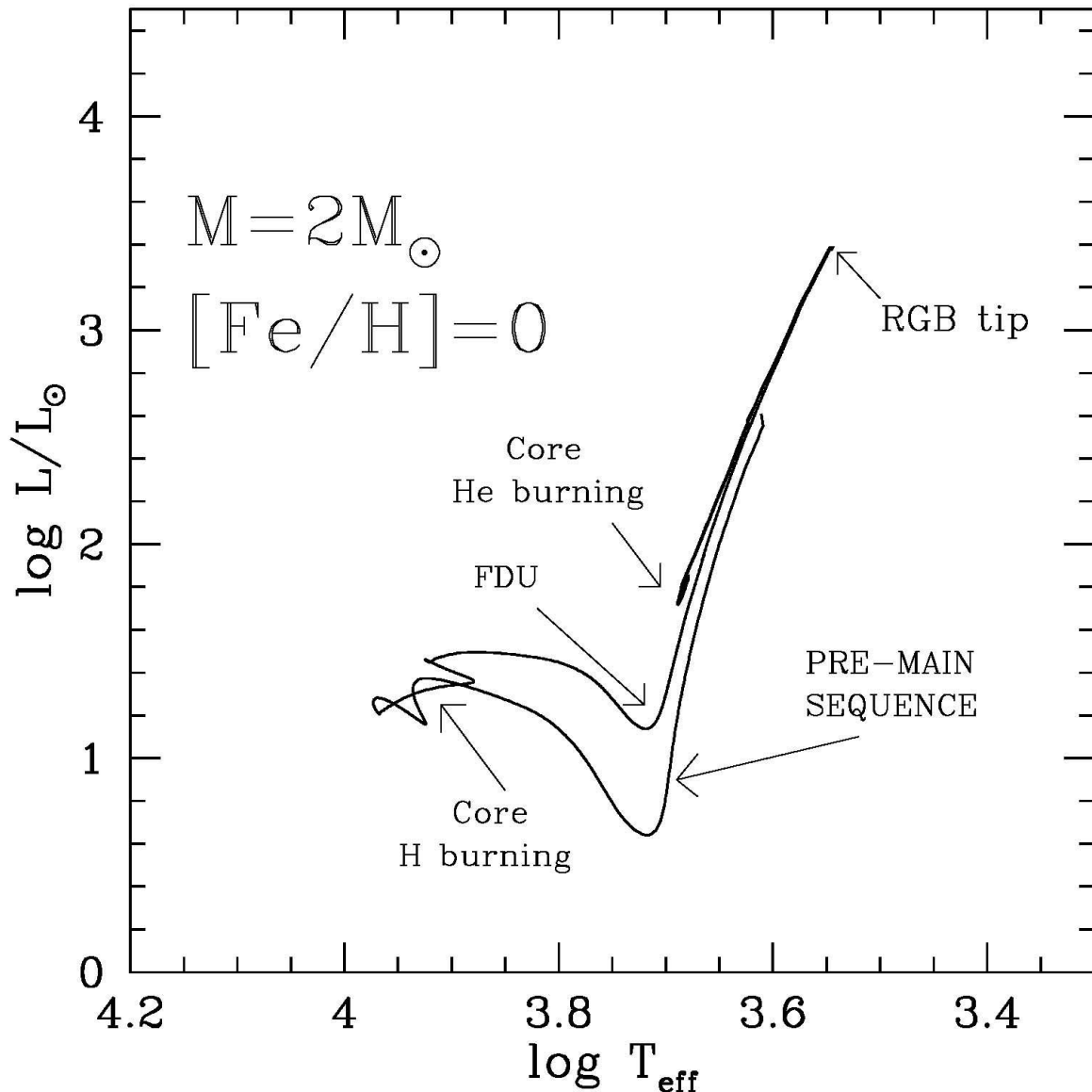
Ventura & Castellani 2005

Case without extramixing remains on the
red side (see also Pietrinferni et al. 2004)

0.9

0.4

AGBs in the theoretical HR diagram



Very luminous

(10^3 - $10^4 L_{\text{SUN}}$)

Very cold

(2000-3000 K)

Synthetic AGB models

Bruzual&Charlot

Groenewegen

Padua (COLIBRI')

Evolutionary AGB models

FUNS (Teramo)

ATON (Roma)

STAREVOL (Bruxelles)

MONSTAR (Monash)

MESA (Victoria; Keele)

Fuel Consumption Theorem

Renzini, Maraston

Why AGBs are so important (1)

OBSERVATIONAL POINT OF VIEW

- **Excellent tracings of halo structures;**
- **IR emission (effects on integrated colors of young-to-intermediate stellar populations);**
- **Unveil the SFR history in resolved stellar populations;**
- **tracers of intermediate age populations (IZw18);**
- **distance indicators (Mira).**

Why AGBs are so important (2)

CHEMICAL POINT OF VIEW

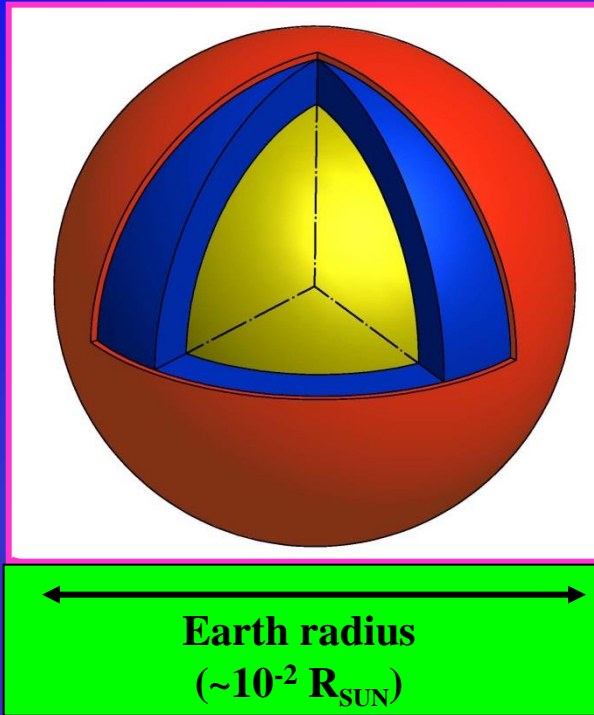
➤ C and N, crucial for organic chemistry and life cycles
(Half of all the observed ^{12}C (?) at least 30% !!

C_{60} and PAHs recently found in post-AGB stars)

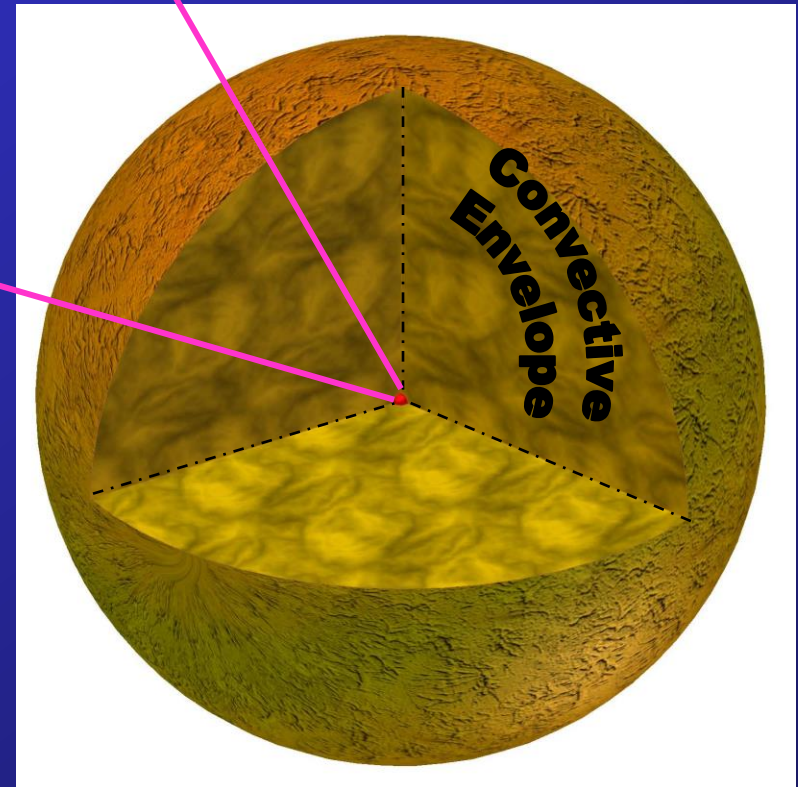
➤ Contamination of the protosolar nebula right before its collapse by a local source AGB or SN (Early Solar System radioactive isotopes)

AGB structure

CO Core
He-shell
H-shell



Earth-Sun
(~200 R_{SUN})



Practically, a nut
in a 300 mts hot air balloon

AGBs: marvellous stellar cauldrons

- C (1.5-4.0 M_{SUN})
- N (4.0-7.0 M_{SUN})
- F (1.5-4.0 M_{SUN})
- Na (all)
- Mg&Al (5.0-7.0 M_{SUN})
- Half of the heavy elements is synthesized in AGBs



Neutron capture reactions

With NO Coulomb barrier to overcome, heavy elements capture neutrons easily even at extremely low energies.

Neutron cross section, in fact, generally INCREASE with decreasing energy

In principle one might expect to encounter astrophysical neutron fluxes spanning over a wide neutron density range.

However, it is one of the fortunate simplifications in neutron capture processes that the most common fluxes are either quite small or quite large.

Neutron capture reactions

With NO Coulomb barrier to overcome, heavy elements capture neutrons easily even at extremely low energies.

Neutron cross section, in fact, generally INCREASE with decreasing energy

The r-process

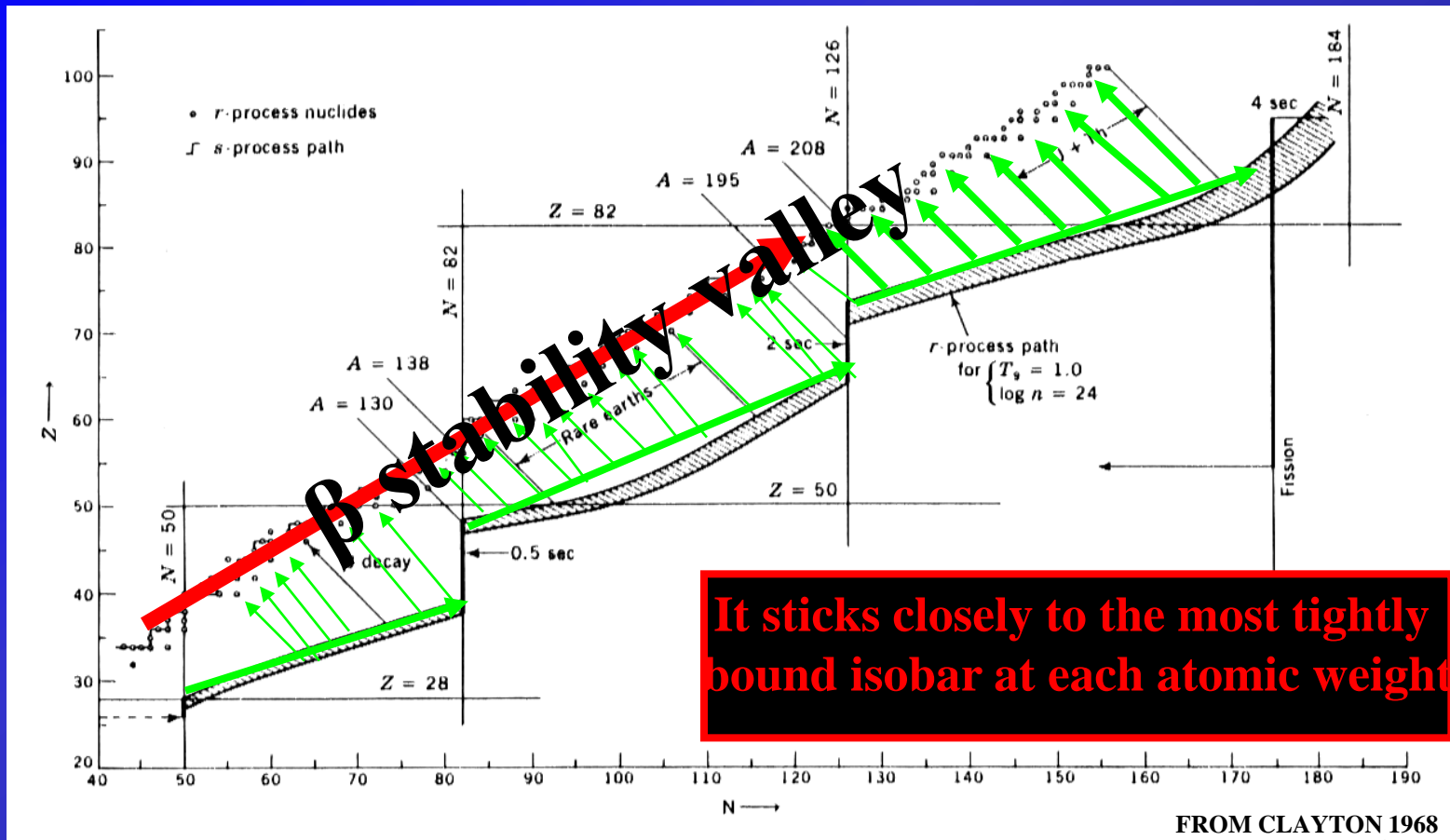
$$\tau_{\beta} \gg \tau_n \quad \Leftrightarrow \quad N_n \sim 10^{20} \text{ n/cm}^3$$

Unstable nucleus captures another neutron before decaying

The s-process

$$\tau_{\beta} \ll \tau_n \quad \Leftrightarrow \quad N_n \sim 10^7 \text{ n/cm}^3$$

Unstable nucleus decays before capturing another neutron



s-process

r-process

Weak component ($A < 90$)

MASSIVE STARS
 Core He-burning
 Shell C-burning

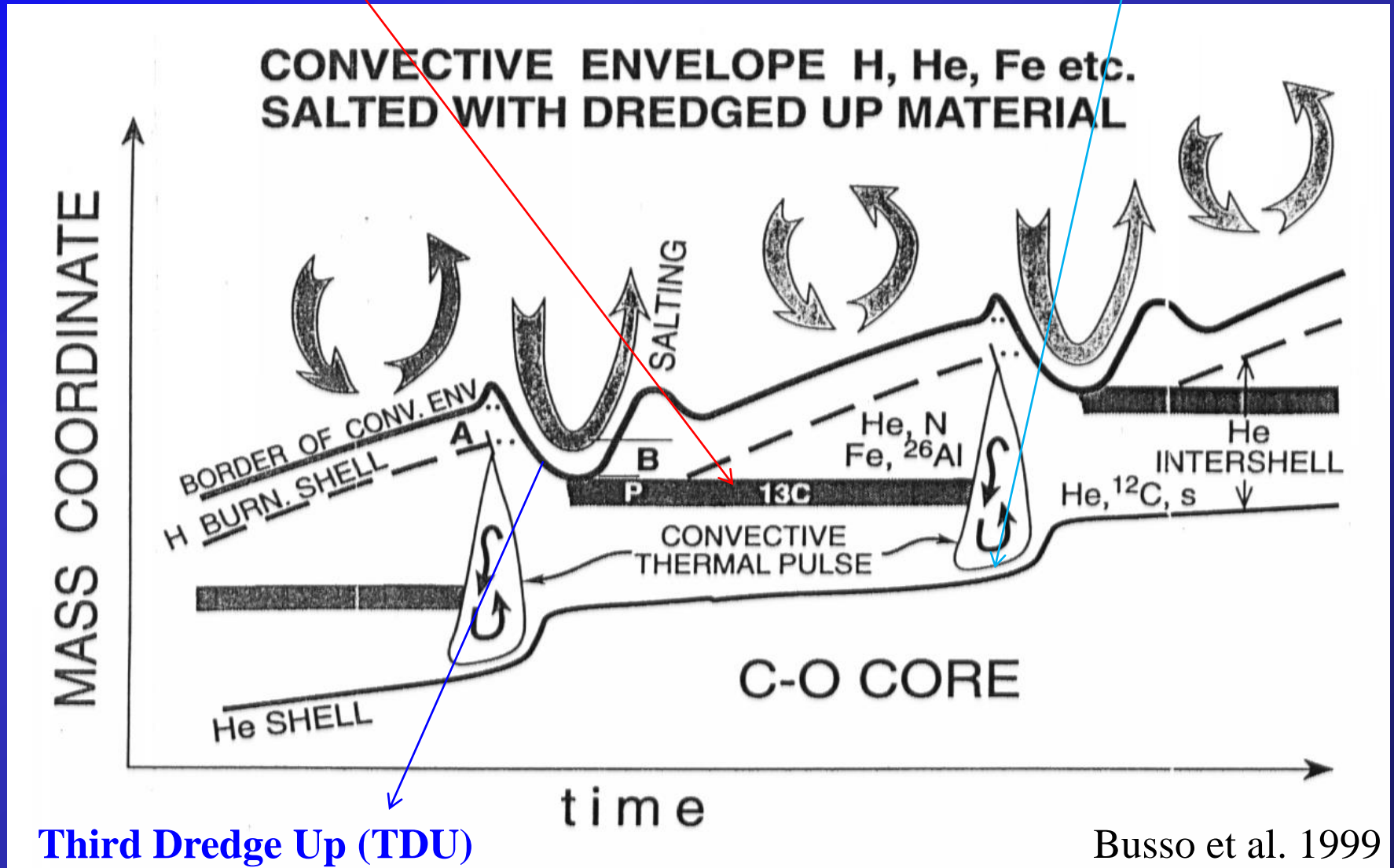
AGB

Main component ($90 < A < 204$)

The s-process in AGB stars

$^{13}\text{C}(\alpha, n)^{16}\text{O}$ reaction

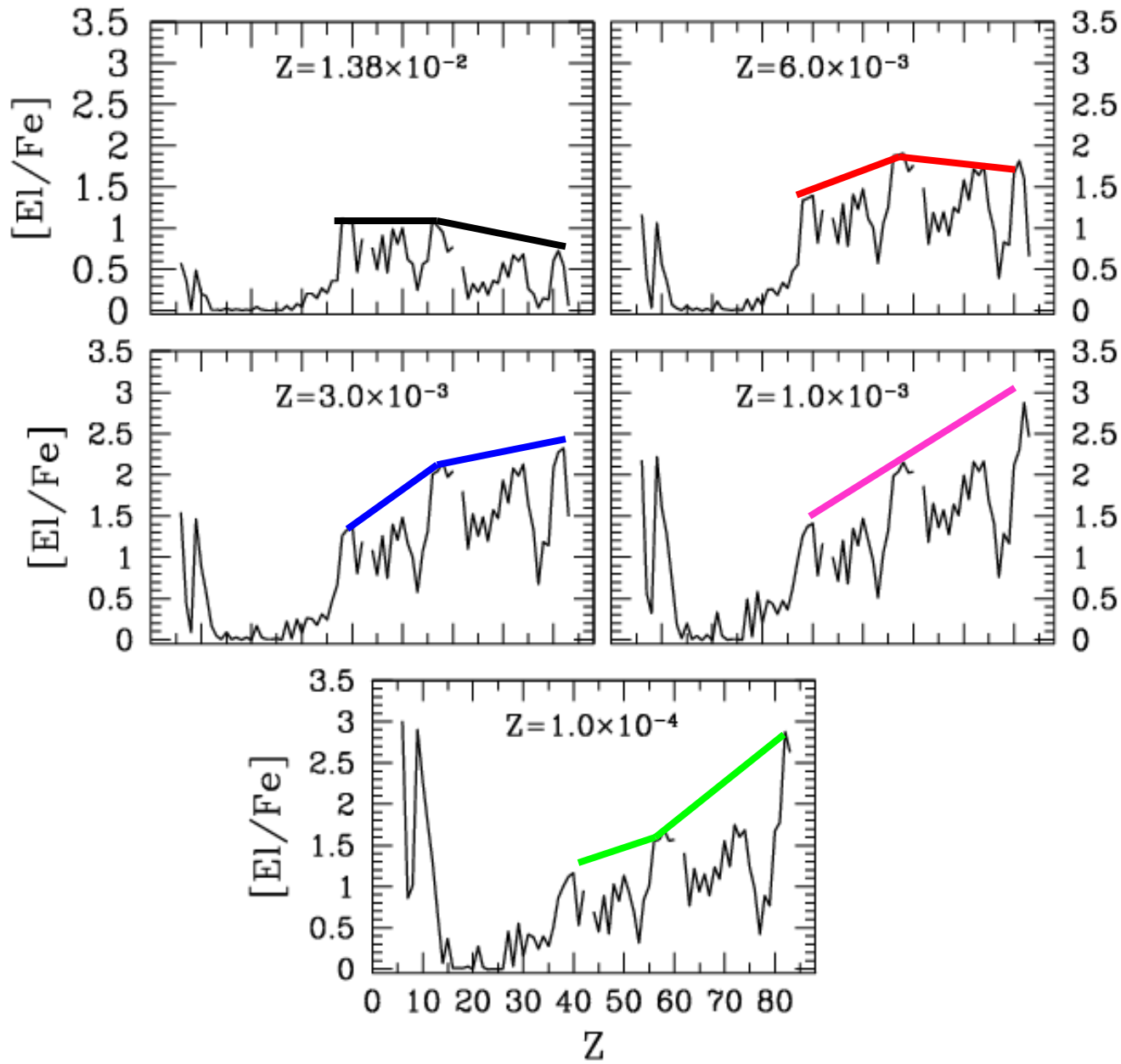
$^{22}\text{Ne}(\alpha, n)^{25}\text{Mg}$ reaction



Third Dredge Up (TDU)

Busso et al. 1999

$M=2M_{\odot}$



Final AGB
composition for
 $0.0001 < Z < Z_{\odot}$

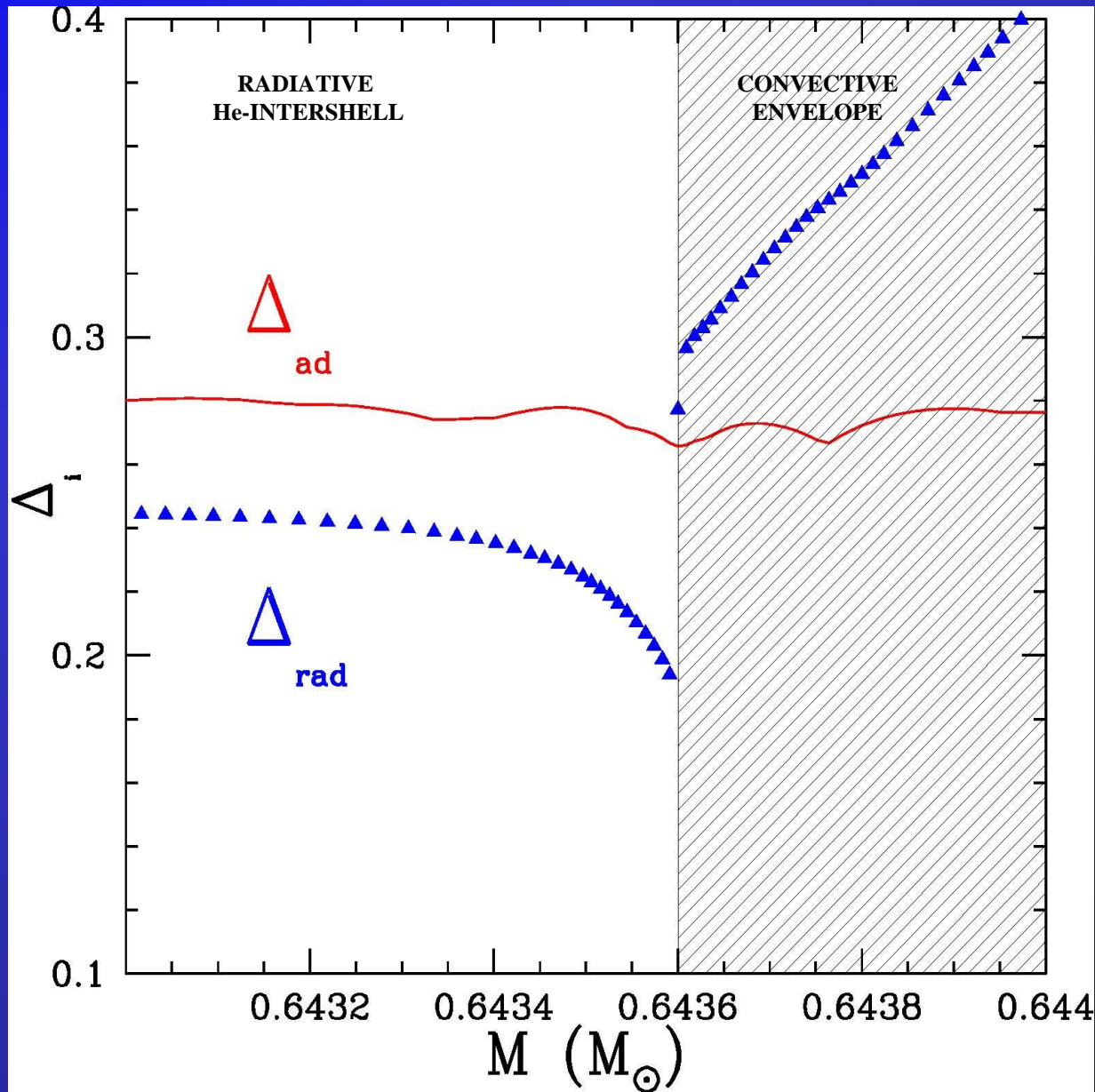
How does the ^{13}C pocket form?

- ✓ **Opacity induced overshoot** (Straniero+ 2006; Cristallo+ 2009)
- ✓ **Convective Boundary Mixing + Gravity Waves** (Battino+ 2017)
- ✓ **Magnetic fields** (Trippella+ 2017)

How does the ^{13}C pocket change?

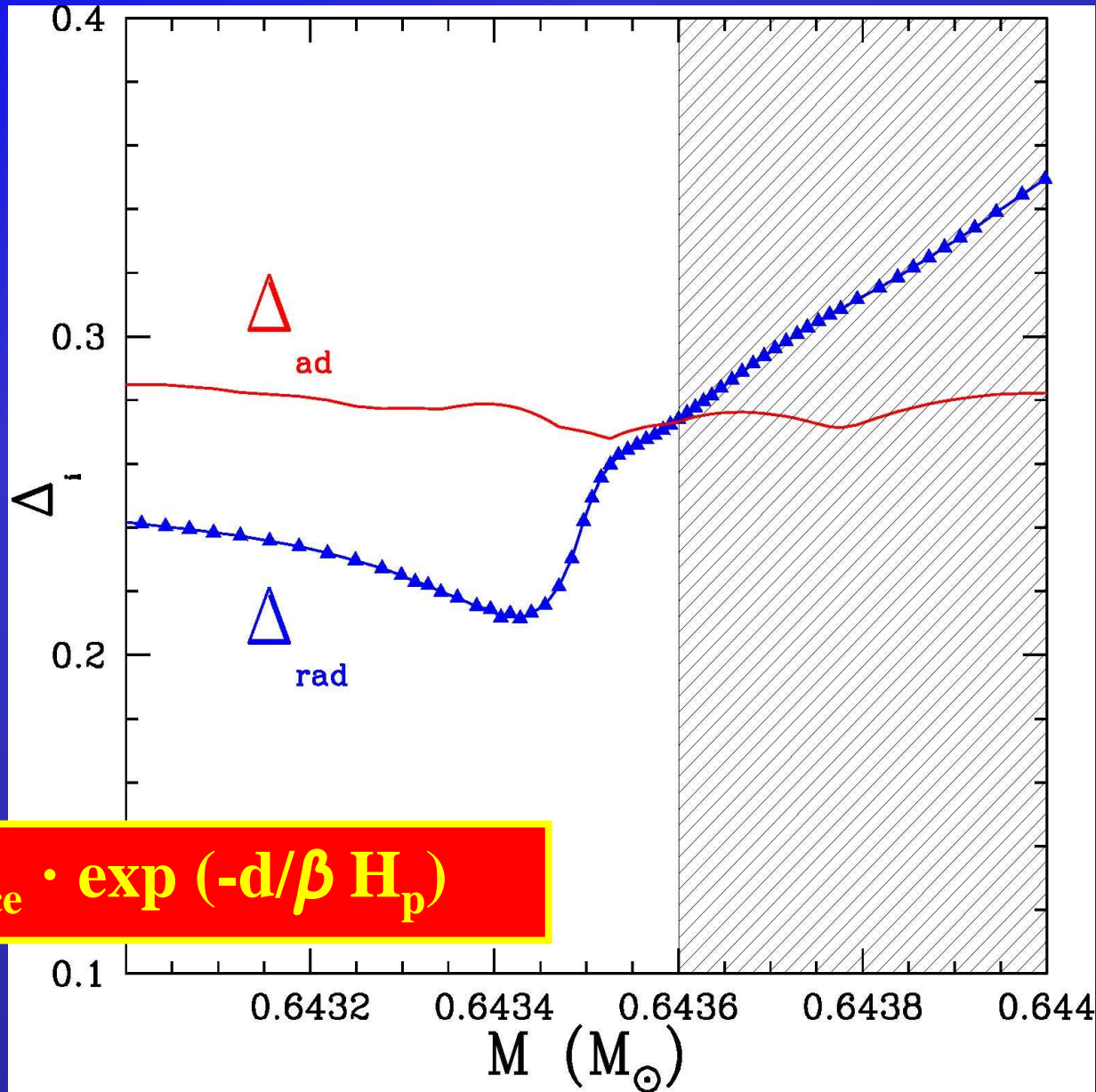
- ✓ **Rotation mixing** (Piersanti+ 2013)
- ✓ **Magnetic fields** (Trippella+ 2017)

Gradients profiles **WITHOUT** exponentially decaying velocity profile



**During
a TDU
episode**

Gradients profiles **WITH** exponentially decaying velocity profile



$$v = v_{\text{bce}} \cdot \exp(-d/\beta H_p)$$

**During
a TDU
episode**

The ^{13}C -pocket and the s-process

Major neutron source

Straniero+ 2006
Cristallo+ 2009,2011

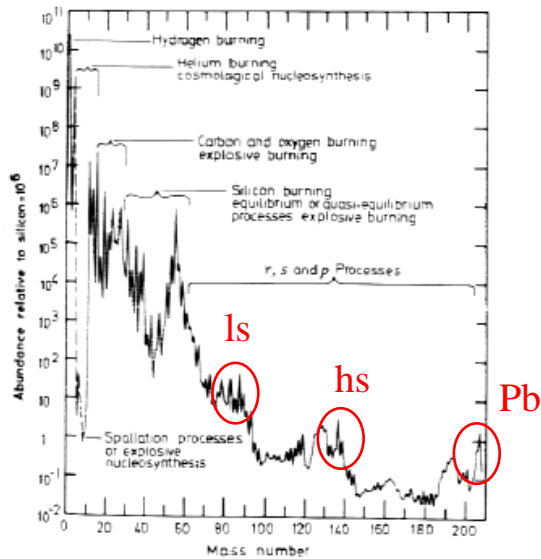
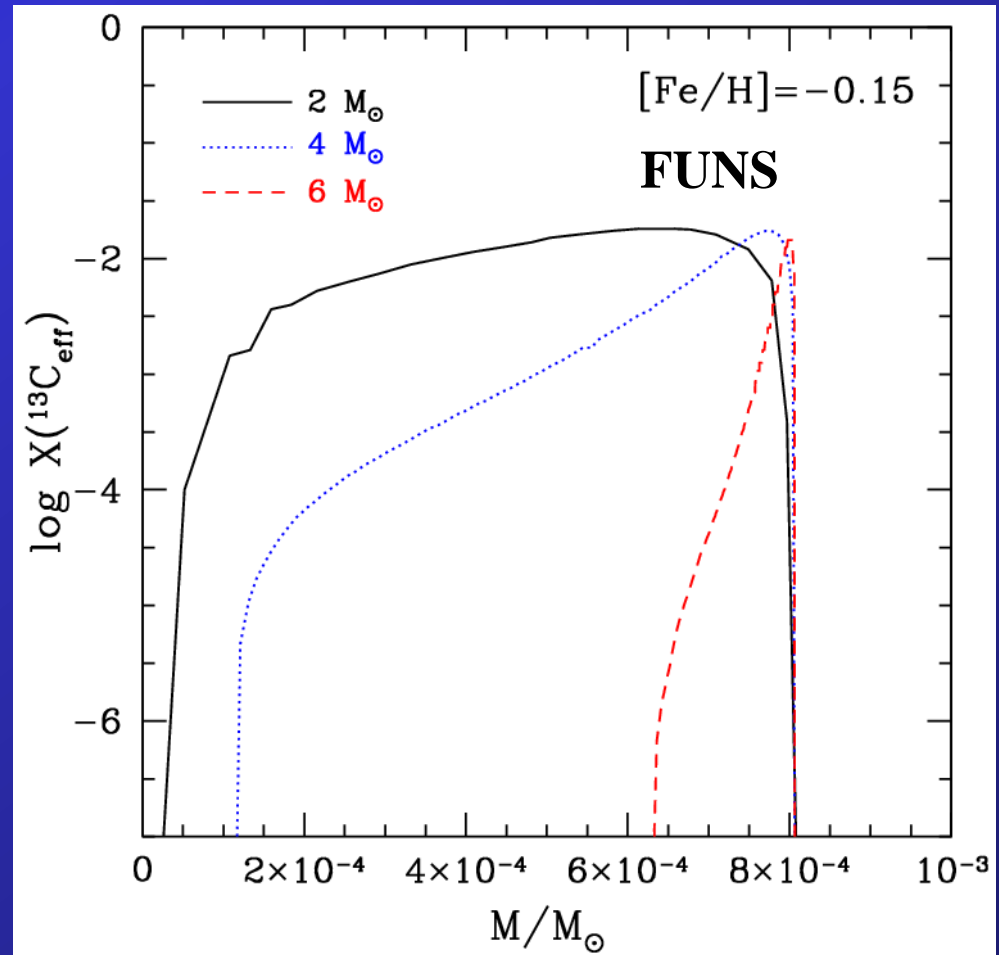


Figure 2.1 Nuclide abundances (relative to $N(\text{Si})=10^6$) as a function of the mass number. Labels in the picture identify different processes responsible for the formation of solar observed isotopes (picture from [40]).



$$[\text{ls}/\text{Fe}] = ([\text{Sr}/\text{Fe}] + [\text{Y}/\text{Fe}] + [\text{Zr}/\text{Fe}]) / 3$$

$$[\text{hs}/\text{Fe}] = ([\text{Ba}/\text{Fe}] + [\text{La}/\text{Fe}] + [\text{Nd}/\text{Fe}] + [\text{Sm}/\text{Fe}]) / 4$$

Comparison between evolutionary codes (I): light and heavy elements

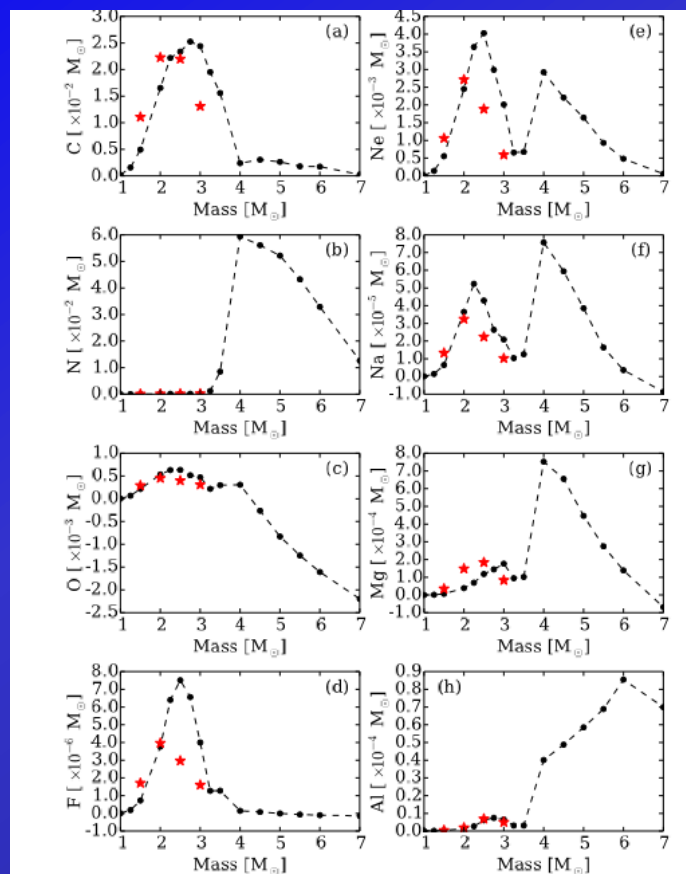


FIG. 11.— Net yields of select elements lighter than Si as a function of initial mass. Results from Cristallo et al. (2011) are shown as red stars.

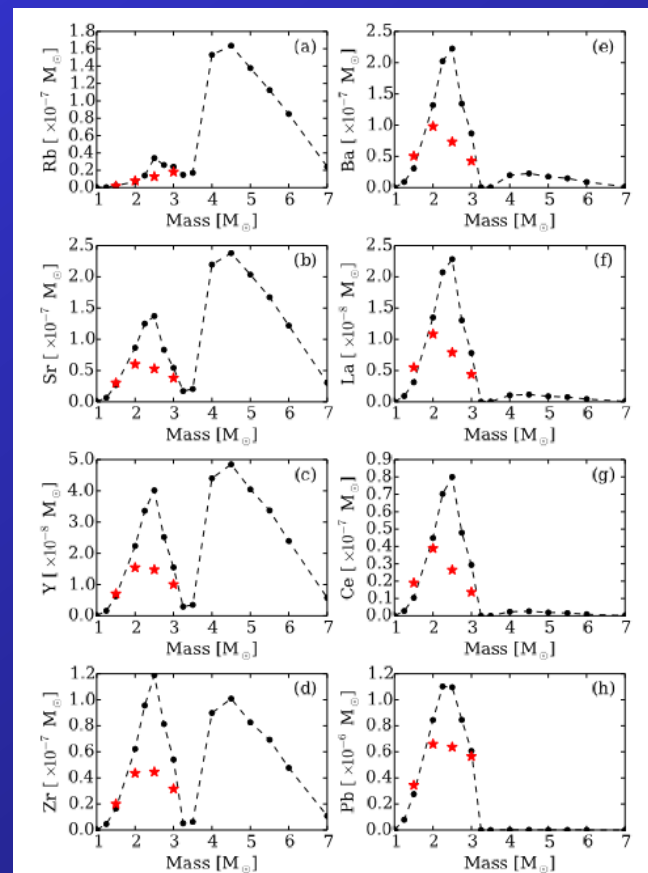


FIG. 13.— Net yields of select neutron-capture elements as a function of initial mass. Results from Cristallo et al. (2011) are shown as red stars.

TDU as a function of mass

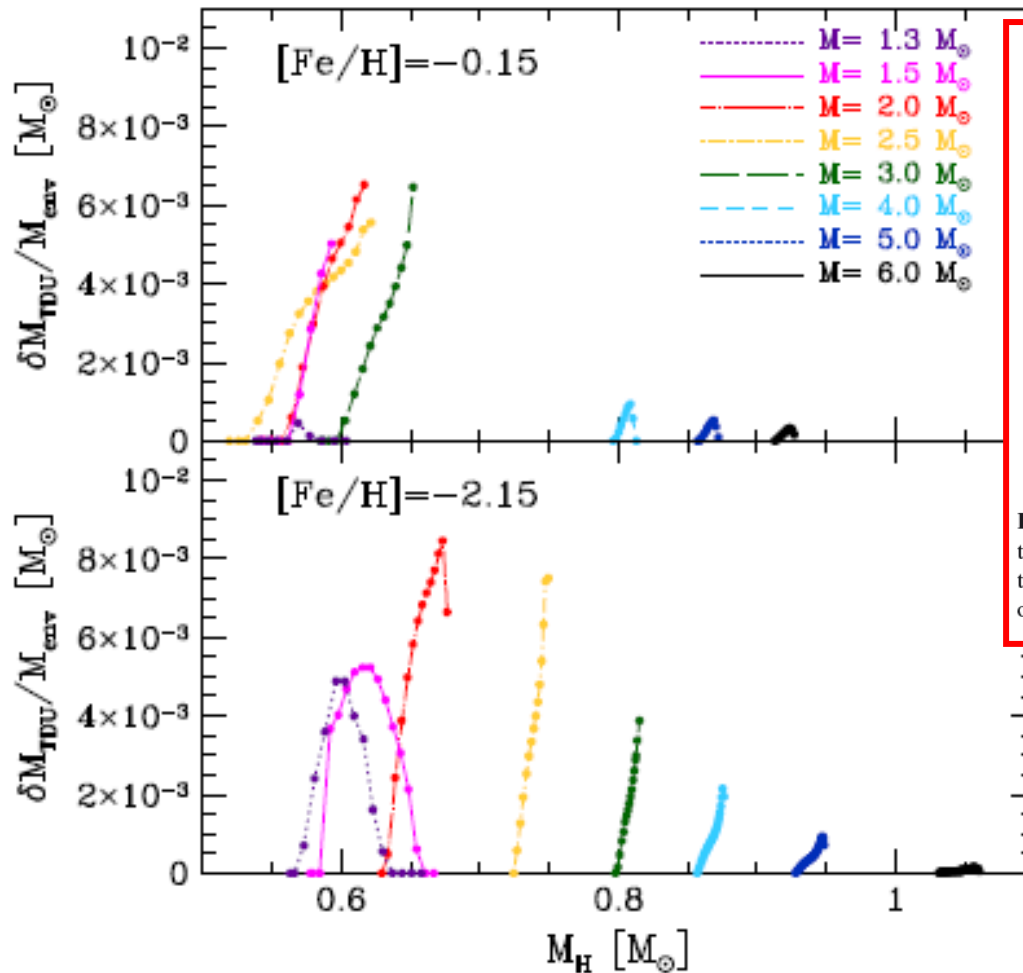


Figure 3. Ratio between the mass of H-depleted dredged-up material (δM_{TDU}) and the envelope mass (M_{env}) for different masses at $Z = 10^{-2}$ (upper panel) and $Z = 2.4 \times 10^{-4}$ (lower panel).

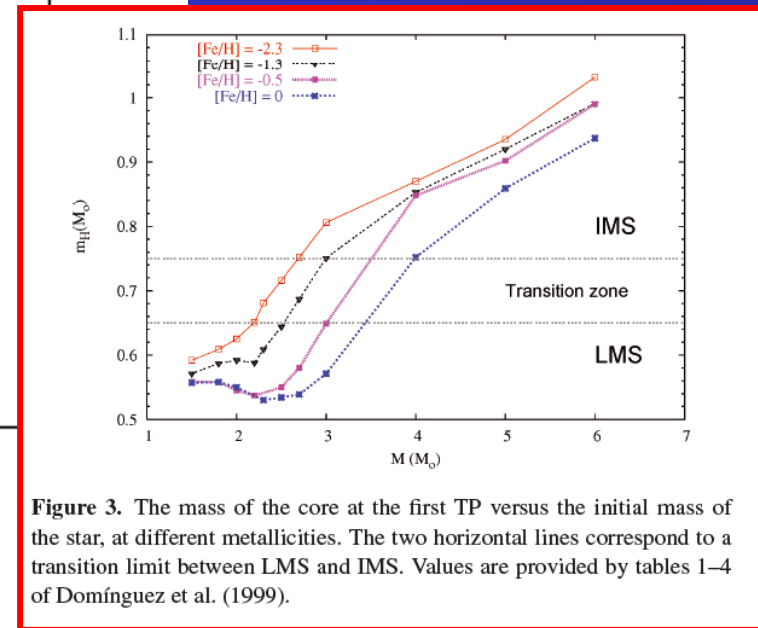
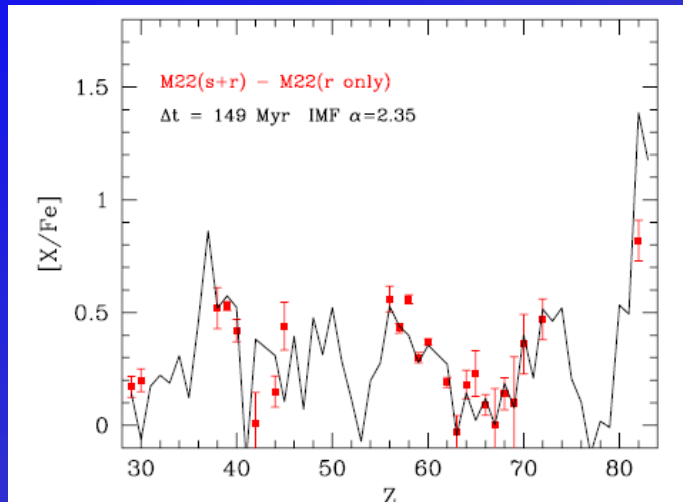


Figure 3. The mass of the core at the first TP versus the initial mass of the star, at different metallicities. The two horizontal lines correspond to a transition limit between LMS and IMS. Values are provided by tables 1–4 of Domínguez et al. (1999).

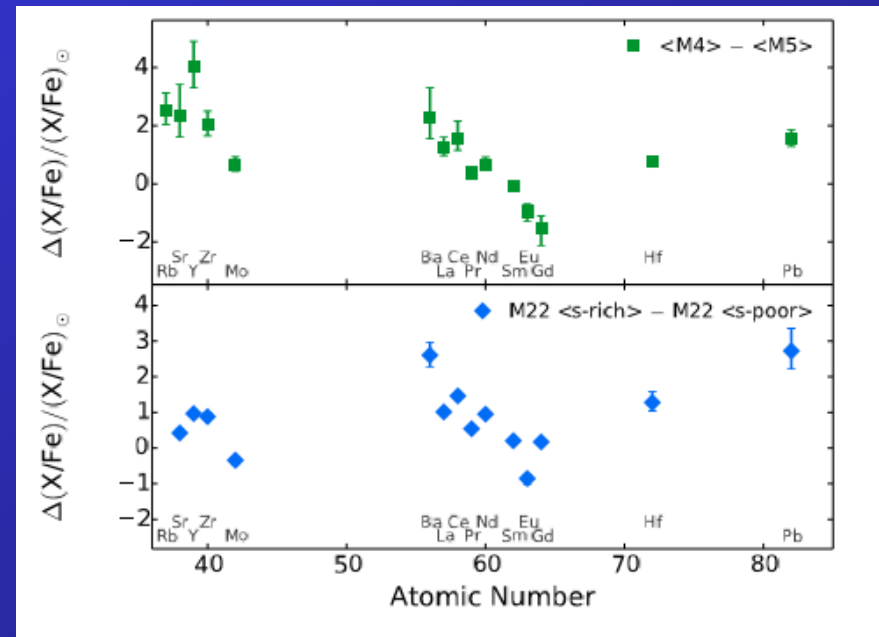
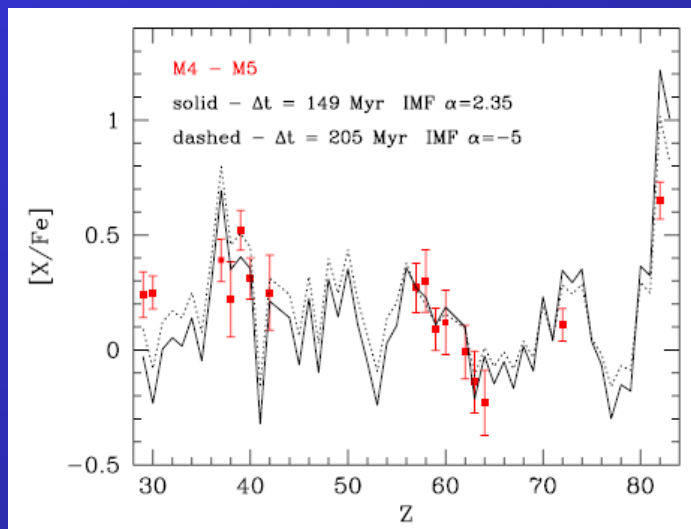
Bisterzo+ 2010

Cristallo+ 2015

s-rich Globular Clusters: the importance of massive AGBs



Straniero+ 2014



Shingles+ 2014

Comparison between evolutionary codes (II): TDU efficiency

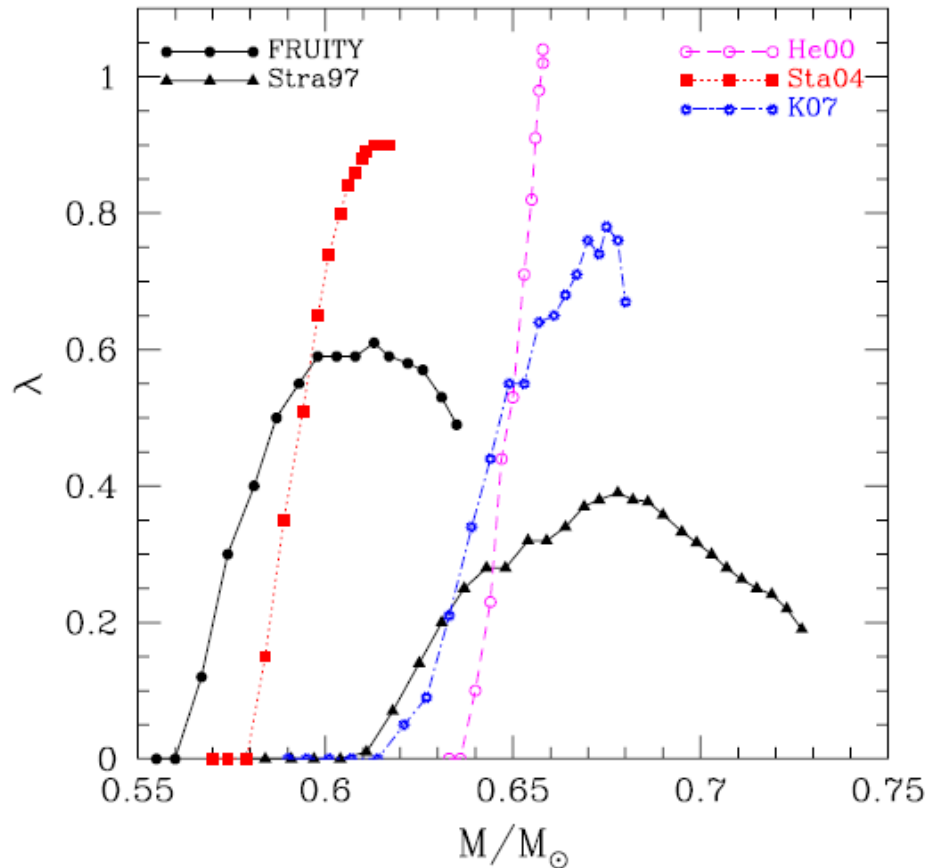
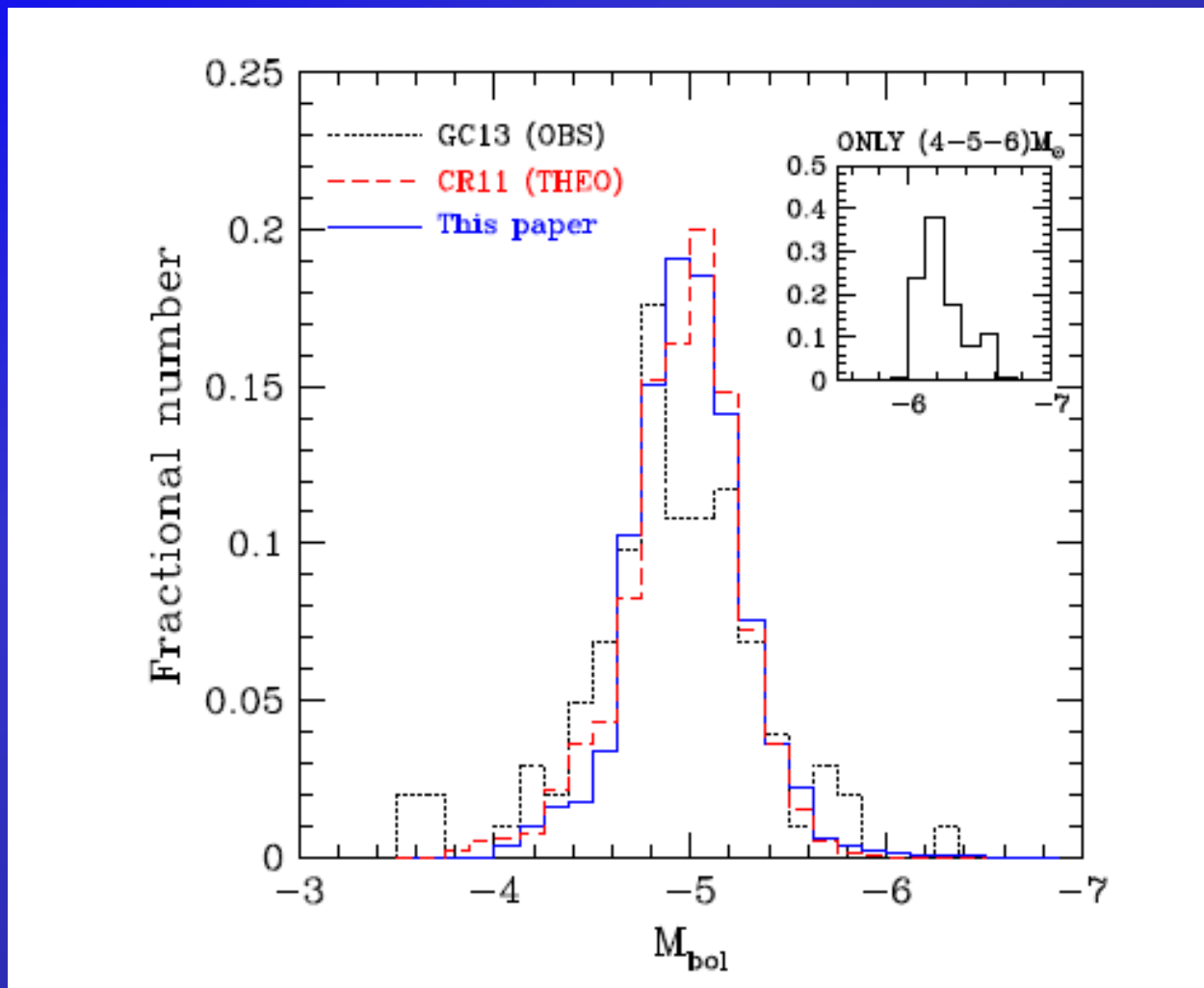


Figure 8. λ factor as a function of the core mass for an AGB model with $M = 3 M_{\odot}$ and $Z = 0.02$ as reported by different authors (FRUITY: this paper; Stra97: Straniero et al. 1997; He00: Herwig 2000; Sta04: Stancliffe et al. 2004; K07: Karakas & Lattanzio 2007).

He \uparrow \rightarrow $M_{\text{ini}}^{\text{AGB}}$ \downarrow
He \uparrow \rightarrow C \downarrow
Karakas+ 2014,15

The Luminosity function of Galactic C-stars



ULTIMATE STEP WITH GAIA!!!!

Comparison between evolutionary codes (III): core masses

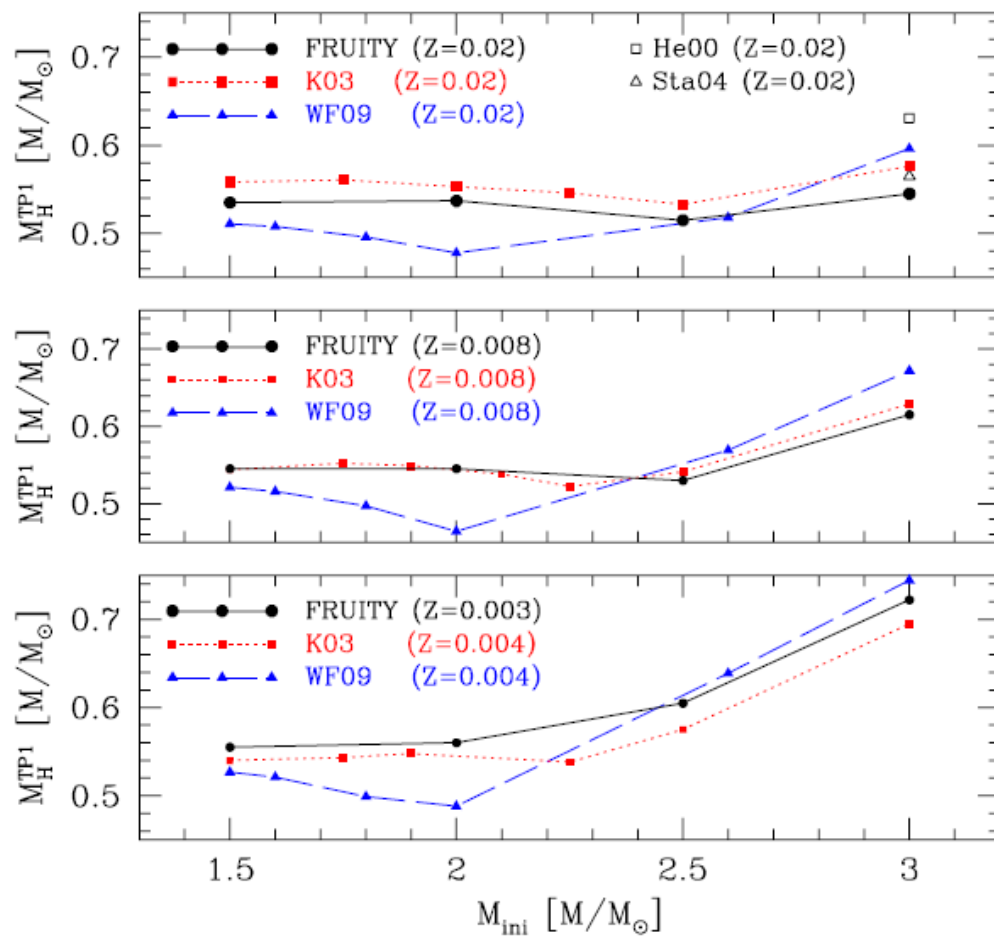


Figure 7. Core mass at the first TP as a function of the initial stellar mass at various metallicities and for different authors (FRUITY: this paper; K03: Karakas 2003; WF09: Weiss & Ferguson 2009; He00: Herwig 2000; Sta04: Stancliffe et al. 2004).

The **Initial-to-Final** mass relation is important for any problem related to the origin and evolution of gas in stellar populations.

It is a crucial quantity to determine the age of stellar populations when using the WD luminosity functions.

Comparison to observations

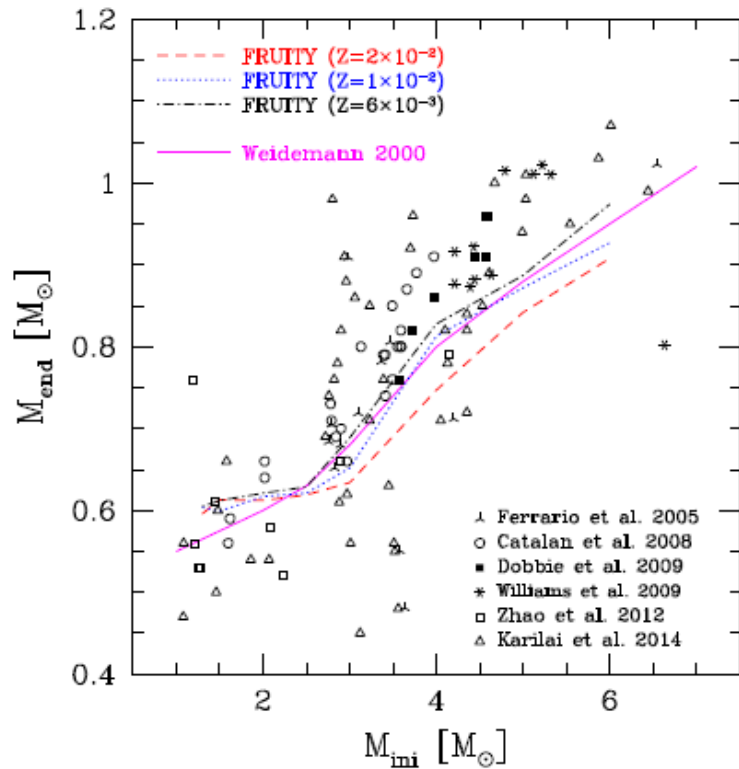
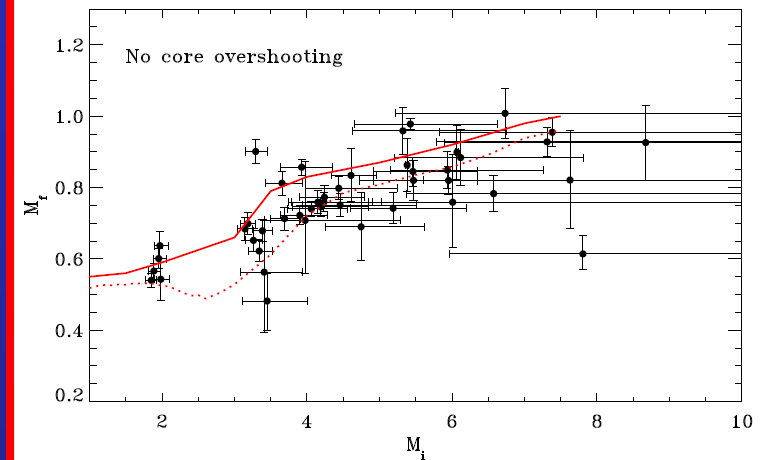
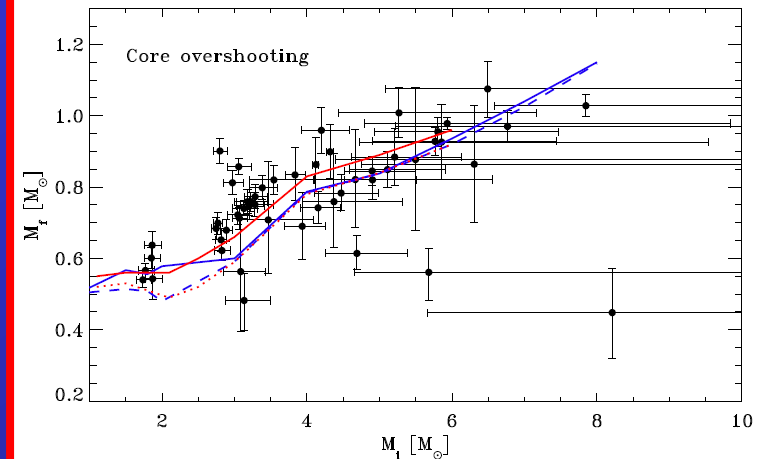


Figure 21. FRUITY models Initial-to-final mass relations for selected metallicities, compared to the semi-empirical relation from Weidemann (2000) and to Open Clusters observations.



Cristallo+ 2015

Salaris+ 2008

PROBLEM: the isochrones employed to determine the age of the cluster should be computed with the same code used to calculate M_{end} .

AVAILABLE AGB YIELDS

MONASH

- **Karakas+ 2003**
- **Karakas+ 2007**
- **Karakas+ 2009**
- **Lugaro+ 2012**
- **Fishlock+ 2014**
- **Shingles+ 2014**
- **Shingles+ 2015**
- **Karakas+ 2016**

TERAMO

- **Cristallo+ 2009**
- **Cristallo+ 2011**
- **Piersanti+ 2013**
- **Straniero+ 2014**
- **Cristallo+ 2015**
- **Cristallo+ 2016**

The FUNS (FULL Network Stellar) Evolutionary Code

(Straniero+ 2006 and references therein; Cristallo+ 2009)

F.R.U.I.T.Y. Database

(FUNS Repository of Updated Isotopic Tables & Yields)

On line at www.oa-teramo.inaf.it/fruity

Cristallo+ 2011,2015,2016
Piersanti+ 2013

Select Data:

Mass (M_{\odot})	Metallicity (Z) ⁽¹⁾	Nuclides Properties	Multiple Table format ⁽⁸⁾	Single Table format ⁽⁹⁾
---	---	<input checked="" type="radio"/> Elements ^(2,3) Z: <input type="text" value="All"/>	<input checked="" type="radio"/> All Dredge Up Episodes ⁽¹⁰⁾	<input type="radio"/> Final Composition
		<input type="radio"/> Isotopes ⁽⁴⁾ A: <input type="text" value="All"/> Z: <input type="text" value="All"/>	<input type="radio"/> Final Composition	
		<input type="radio"/> s-process ⁽⁵⁾ : [hs/ls], [Pb/hs], ...		
		<input type="radio"/> Net ⁽⁷⁾		
		Yields ⁽⁶⁾ A: <input type="text" value="All"/> Z: <input type="text" value="All"/>	<input type="radio"/> Final	<input type="radio"/> Final
		<input type="radio"/> Total		

Don't Show / Only files

Masses[M_{SUN}]: 1.3 – 1.5 – 2.0 – 2.5 – 3.0 - 4.0 – 5.0 - 6.0

[Fe/H]: -2.85, -2.45, -2.15, -1.67 , -1.15, -0.67, -0.37, -0.24, -0.15, 0, +0.15

$v_{\text{ROT}}^{\text{ZAMS}} = 0 - 10 - 30 - 60$ km/s

F.R.U.I.T.Y.

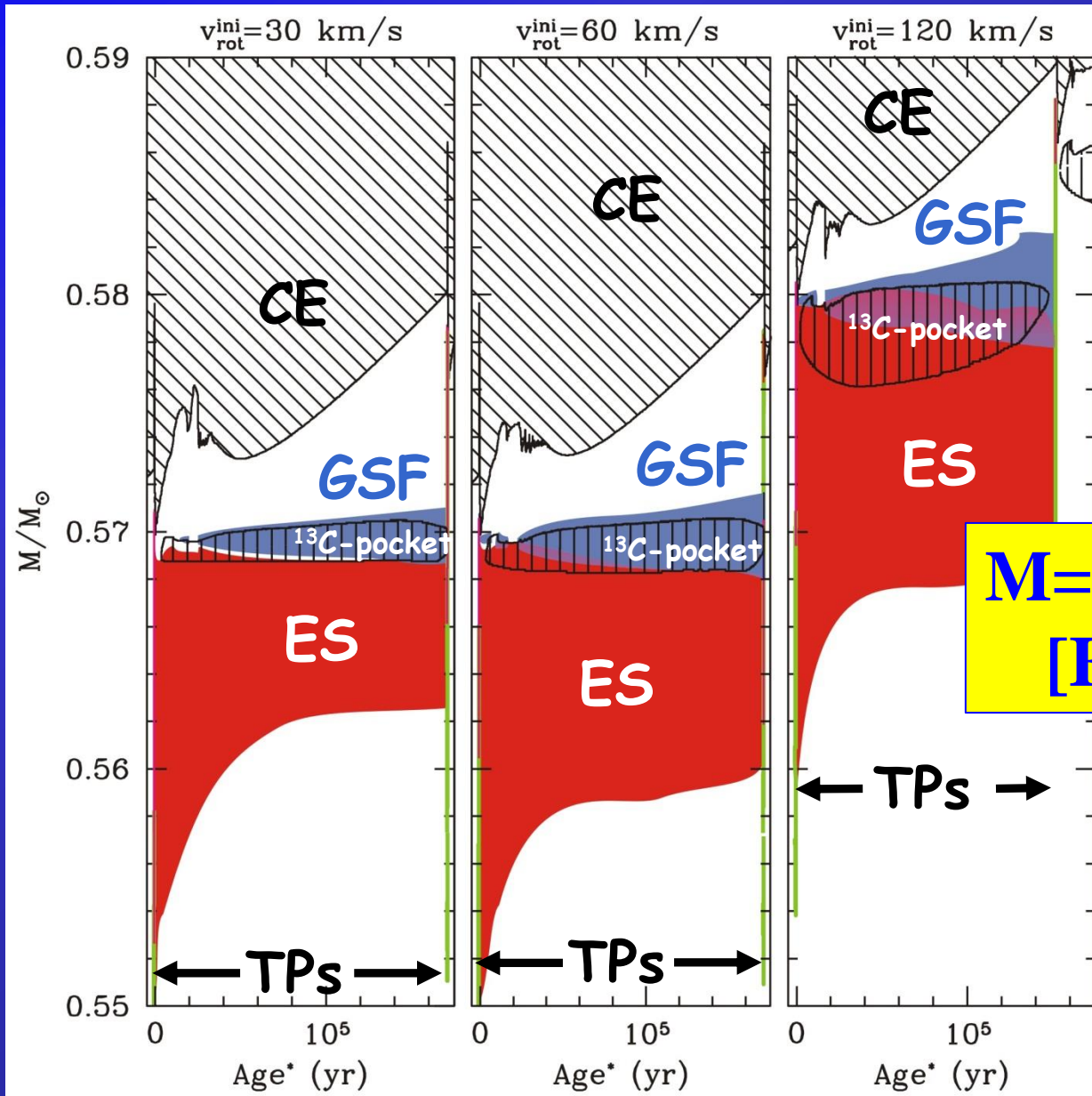
(FULL-Network Repository of Updated Isotopic Tables & Yields)

Select Data:

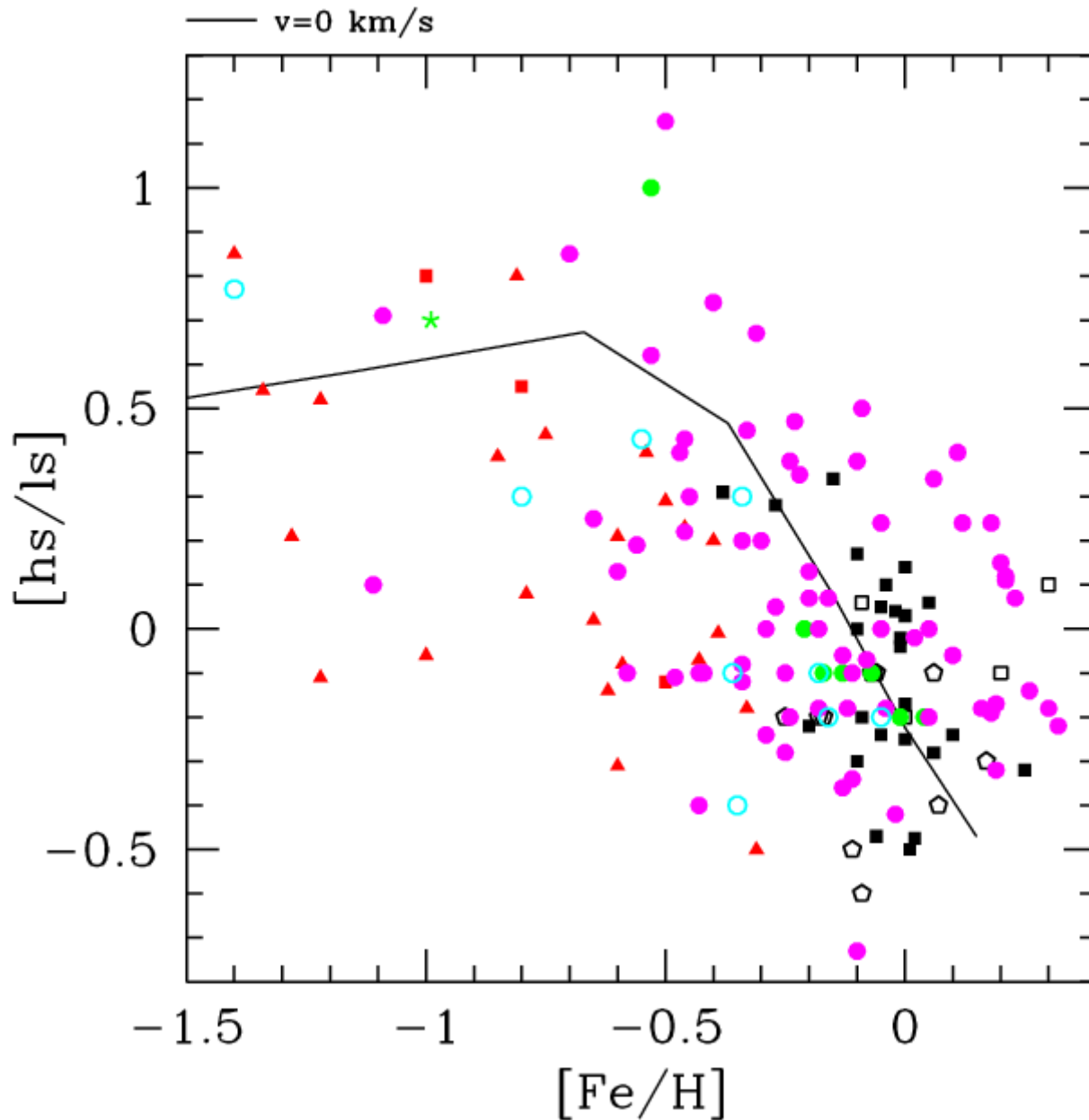
MODEL SELECTION	OUTPUT SELECTION	OUTPUT FORMAT	
Mass (M_{\odot}) ---	Physical Properties	Multiple Table format (14)	Single Table format (15)
Metallicity (Z)⁽¹⁾ ---	Age ⁽³⁾ <input type="checkbox"/> Δt_{ip} ⁽⁴⁾ <input type="checkbox"/>	All TPs <input type="radio"/>	Last TP ⁽¹⁶⁾ <input checked="" type="radio"/>
Initial Rotational Velocity (IRV)⁽²⁾ 0	M_{TOT} ⁽⁵⁾ <input type="checkbox"/> M_H ⁽⁶⁾ <input type="checkbox"/>		Extra ⁽¹⁷⁾ <input checked="" type="radio"/>
¹³C Pocket⁽¹³⁾ Standard	δM_{TDU} ⁽⁷⁾ <input type="checkbox"/> λ ⁽⁸⁾ <input type="checkbox"/>		
	T_{TP}^{max} ⁽⁹⁾ <input type="checkbox"/> M_{bol} ⁽¹⁰⁾ <input type="checkbox"/>		
	$\log(T_{EFF})$ ⁽¹¹⁾ <input type="checkbox"/> $\log(g)$ ⁽¹²⁾ <input type="checkbox"/>		
	<input type="button" value="Select All"/> <input type="button" value="Remove All"/>		

[NOTES ON THE MODELS \(pdf file\)](#)

Rotation induced instabilities during the AGB phase



s-process indexes without rotation: [hs/ls]



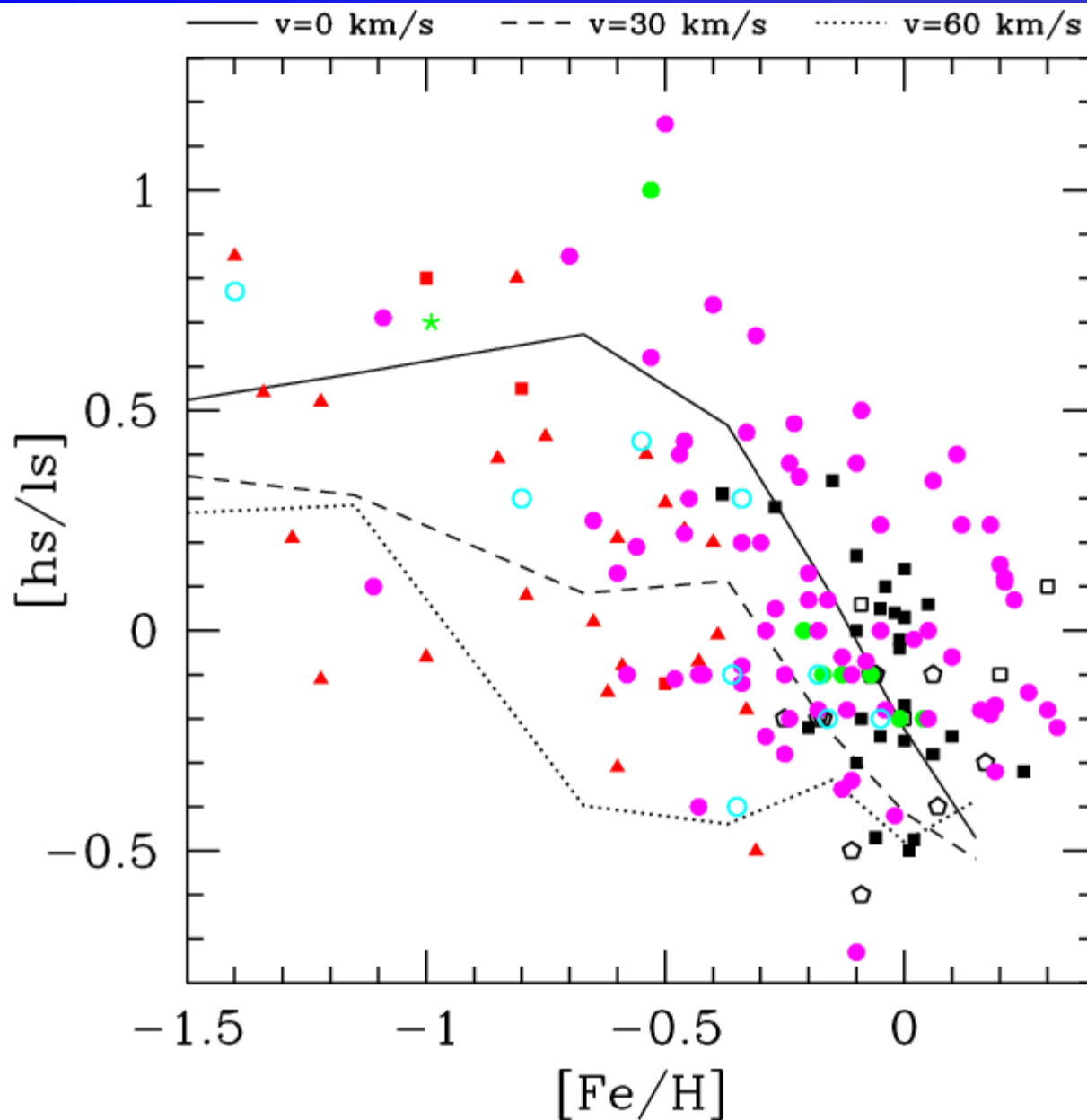
○+● Ba & CH stars

▲ Post-AGBs

■+■ Intrinsic C-rich

●+⬠ Intrinsic O-rich

s-process indexes with rotation: [hs/ls]



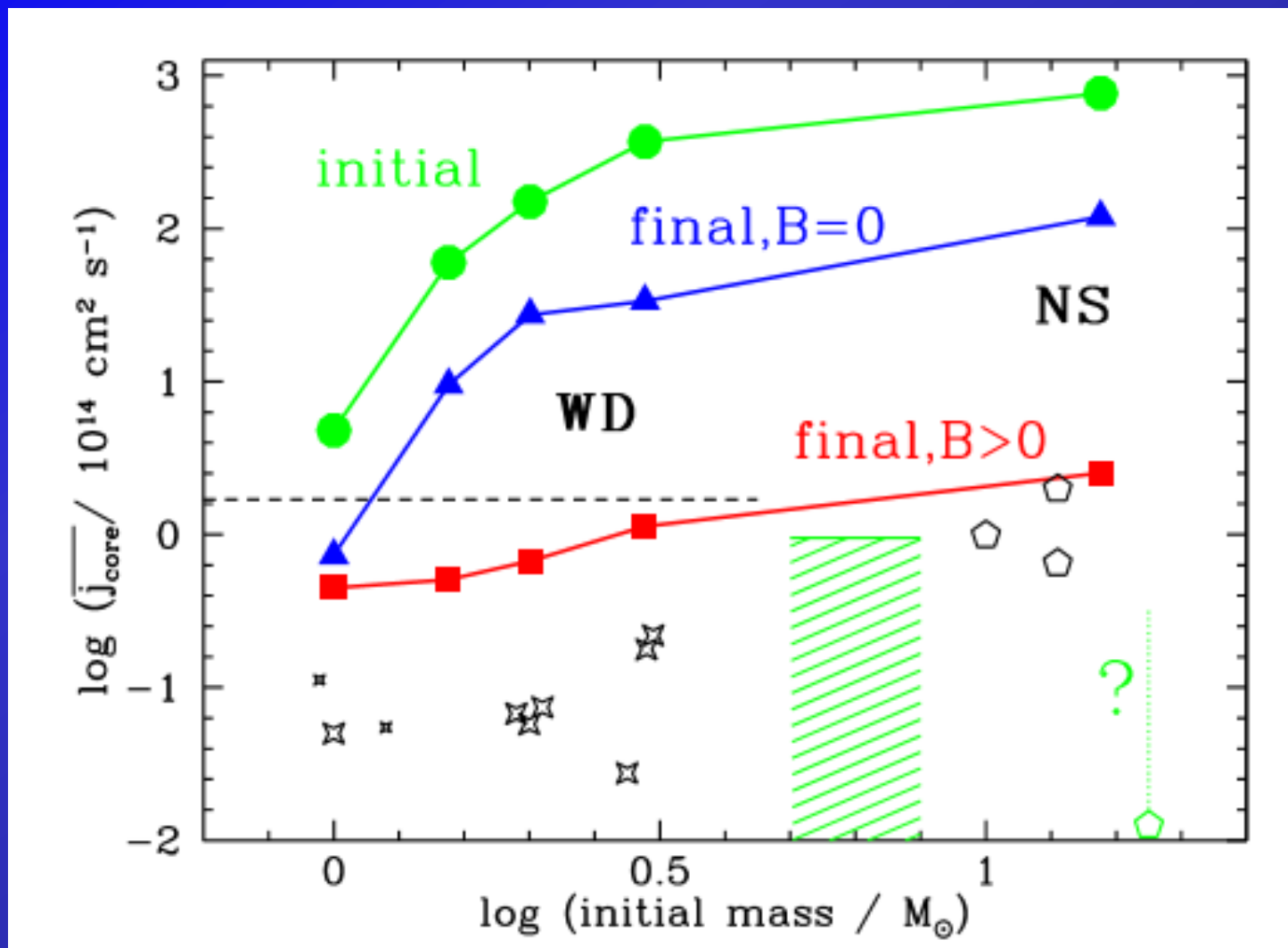
○ + ● Ba & CH stars

▲ Post-AGBs

■ + ■ Intrinsic C-rich

● + ⬠ Intrinsic O-rich

Core specific angular momentum of evolved stars



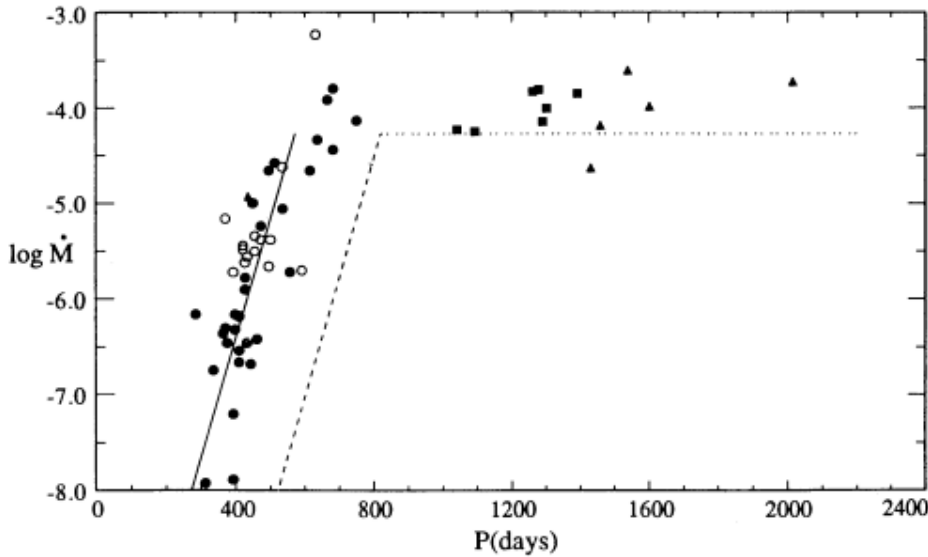
Mass loss law

UP TO EARLY-AGB
PHASE

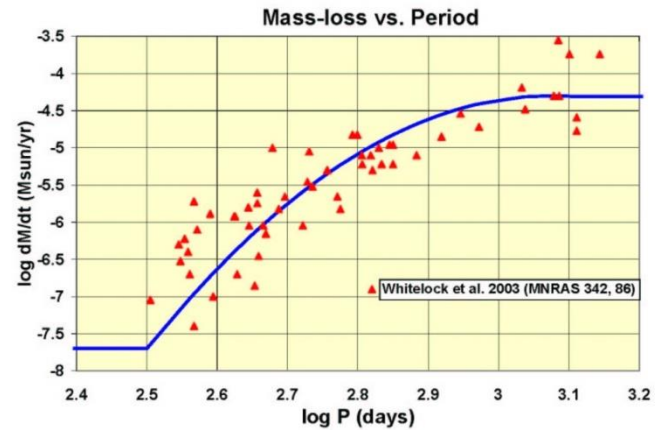


REIMERS MASS-LOSS
($\eta=0.4$)

AGB PHASE

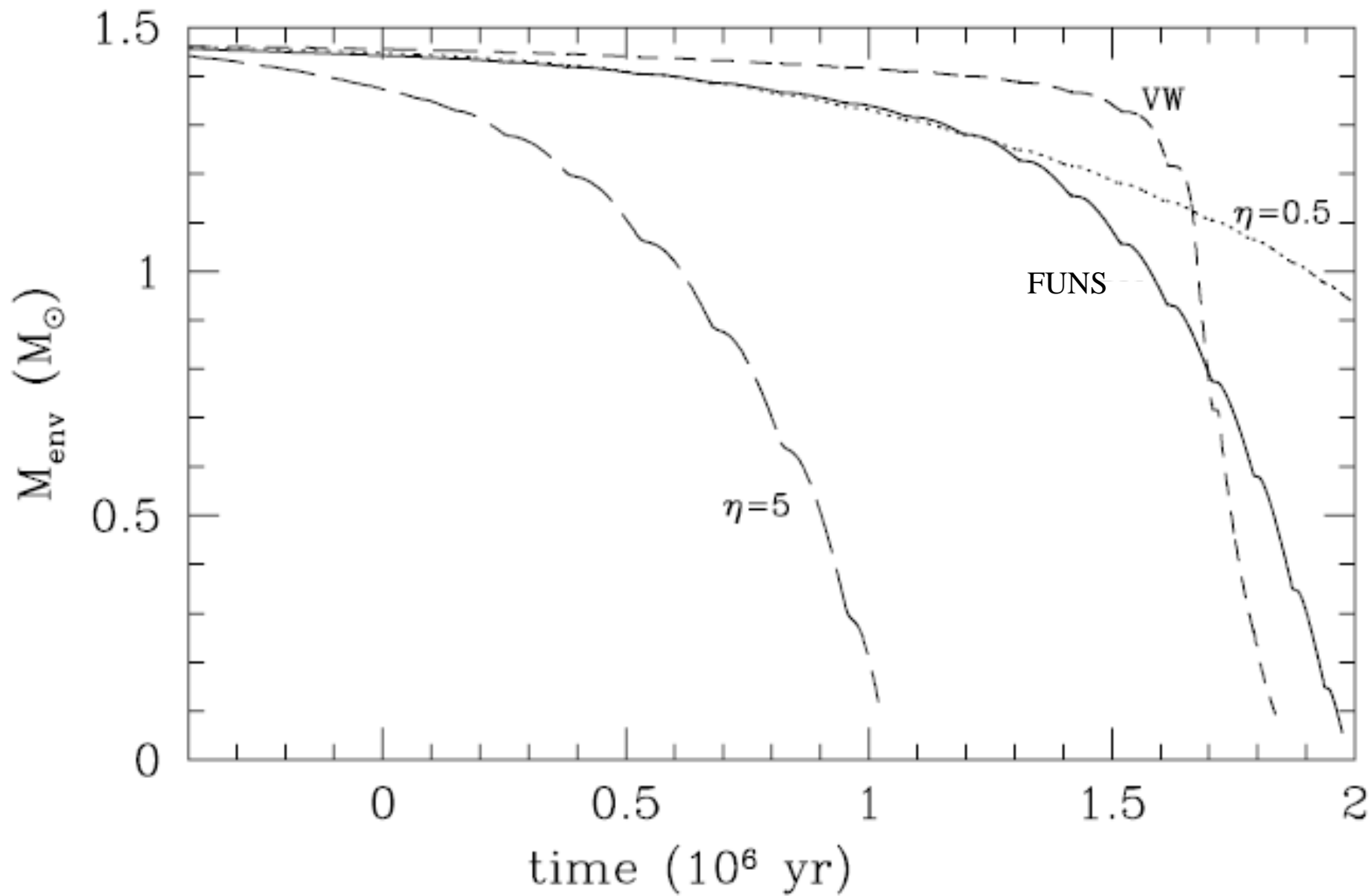


Vassiliadis & Wood 1993

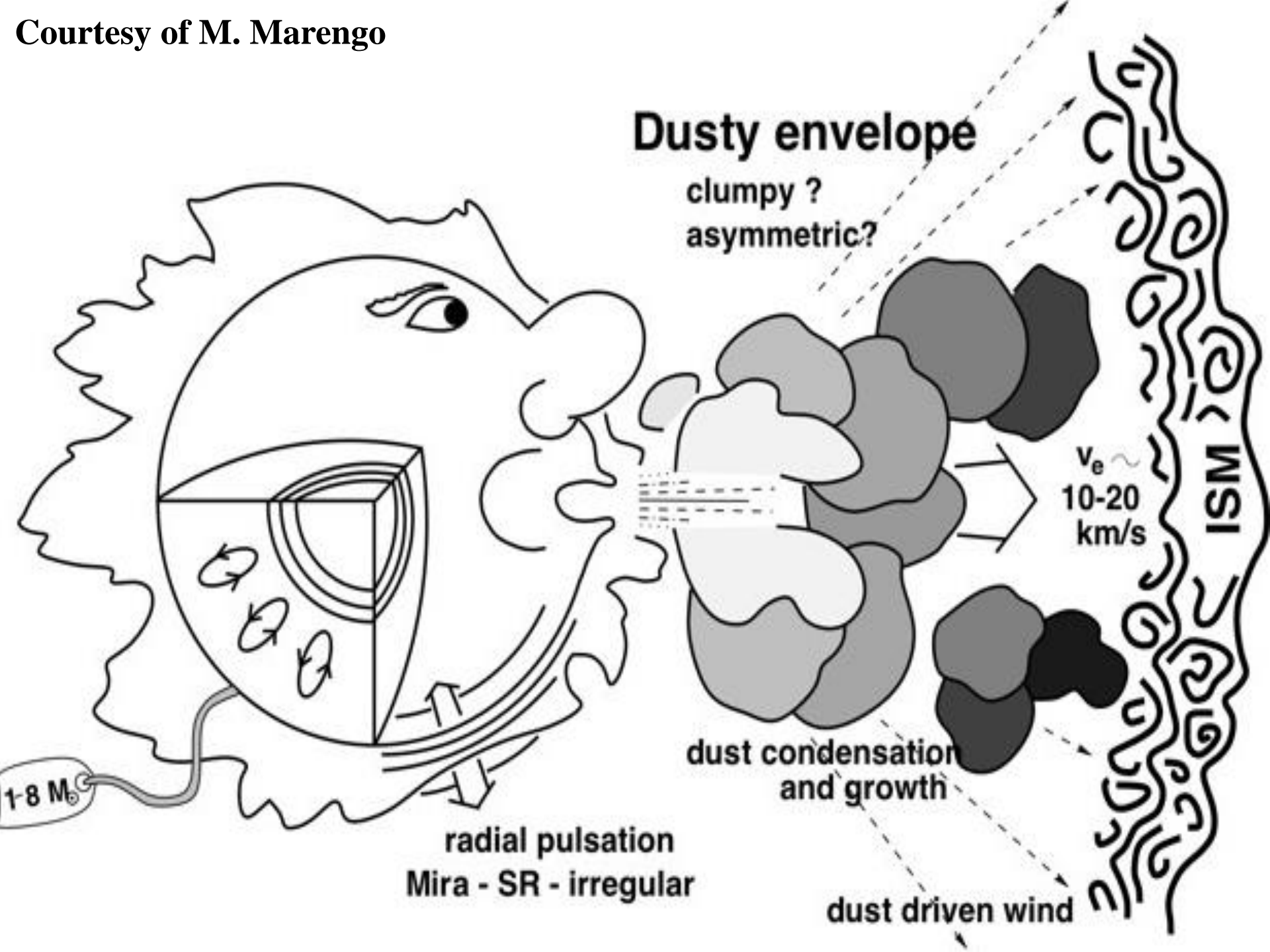


Straniero+ 2006

Mass loss law

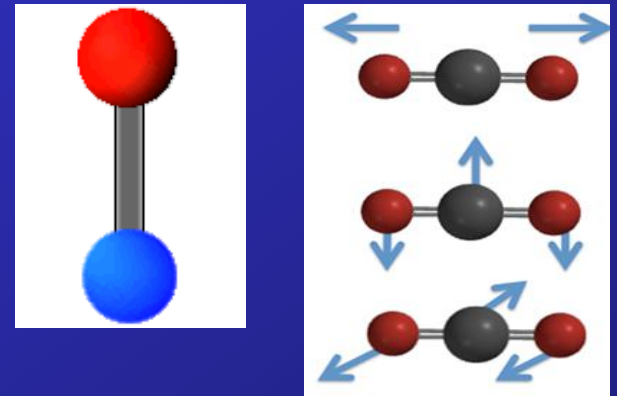


Courtesy of M. Marengo

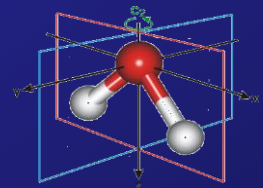
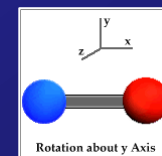
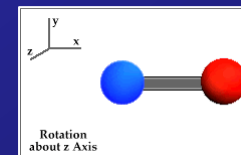


Molecule detection in AGB winds


- vibrational transitions: $\lambda = 0.0003 - 0.03 \text{ cm}$
- \rightarrow probe the inner wind (1-10 R^*)
- characterized by $T \sim 500 - 2500 \text{ K}$
- and densities above 10^6 cm^{-3}



- rotational transitions: $\lambda = 0.3 - 30.0 \text{ cm}$
- \rightarrow found in the intermediate and outer envelope (10-100 R^*) with $T < 500 \text{ K}$
- and $n < 10^6 \text{ cm}^{-3}$



Dust detection in AGB winds

- Spectral features in the micron-range:
- 3 – 8 μm features indicates the presence of PAHs including a plateau at 3.3 – 3.6 μm
- 9.7 / 18 μm O-Si-O bending / stretching mode typical for silicates
- 11.3 μm silicon carbide (SiC) 
- 30 μm feature attributed to MgS dust
- 69 μm silicates of olivine type (e.g. forsterite)

DUST as a candidate to trigger the stellar mass-loss

A&A 514, A35 (2010)

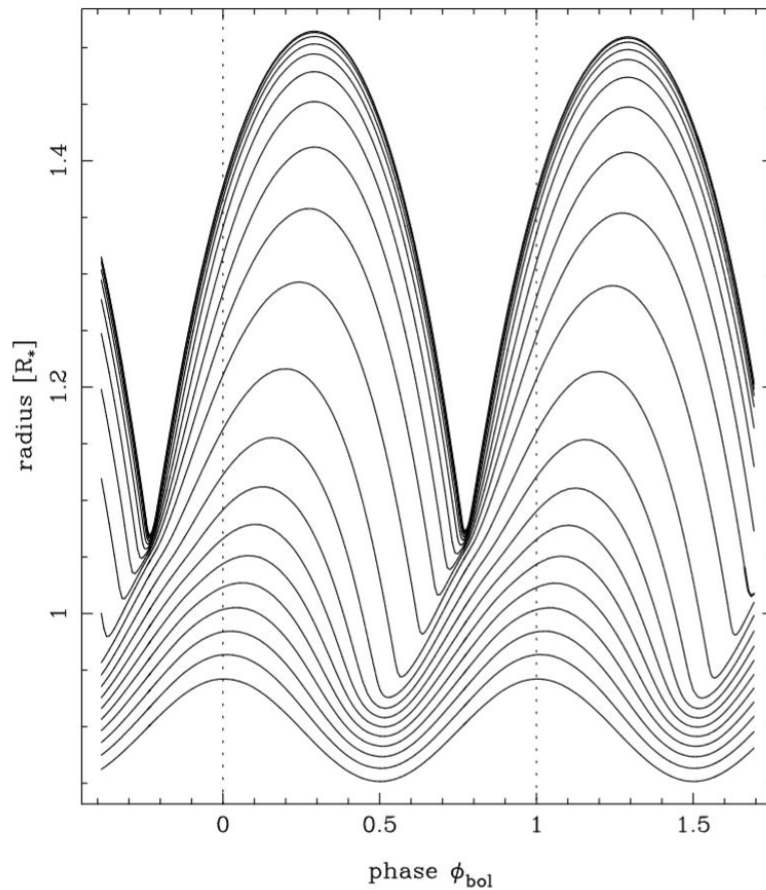


Fig. 1. Movement of mass shells with time at different depths of the dust-free model W, which exhibits no mass loss and shows a strictly periodic behaviour for all layers. Note the different scales on the radius-ordinates compared to Fig. 2. The shown trajectories represent the points of the adaptive grid at a selected instance of time (higher density of points at the location of shocks) and their evolution with time (cf. the caption of Fig. 2 in DMA3 for further explanations).

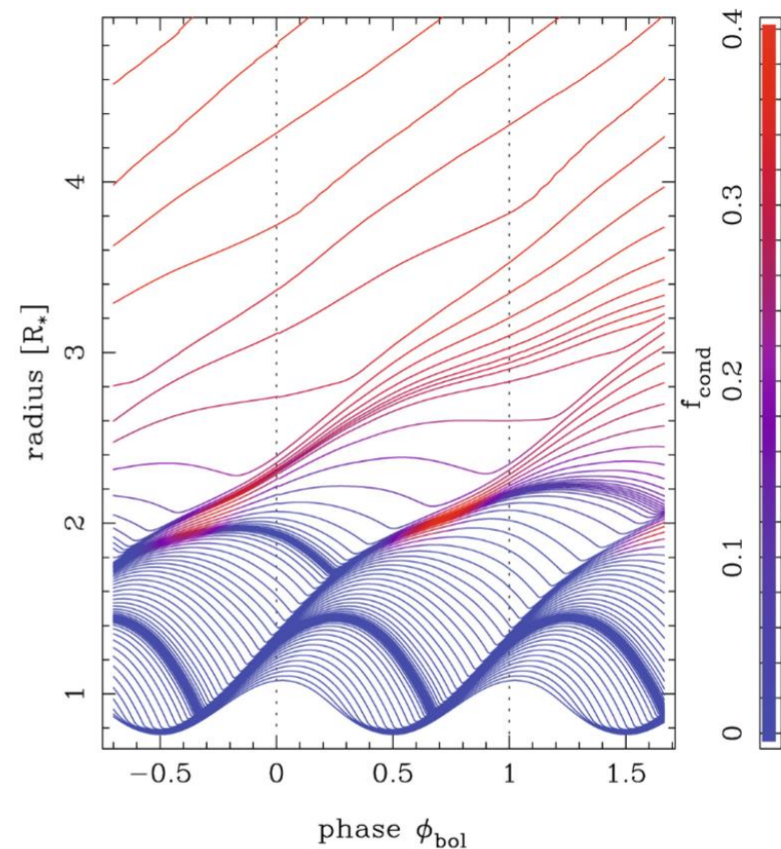


Fig. 2. Same plot as Fig. 1 for model M, representing the scenario of a pulsation-enhanced dust-driven wind. The plot illustrates the different regions within the atmosphere of a typical mass-losing LPV. The innermost, dust-free layers below $\approx 2 R_{\star}$ are subject to strictly regular motions caused by the pulsating interior (shock fronts). The dust-forming region (colour-coded is the degree of dust condensation f_c) at $\approx 2-3 R_{\star}$ where the stellar wind is triggered represents dynamically a transition region with moderate velocities, not necessarily periodic. A continuous outflow is found from $\approx 4 R_{\star}$ outwards, where the dust-driven wind is decisive from the dynamic point of view.

THANK YOU!